



Cite this: *Chem. Soc. Rev.*, 2015,  
44, 5981

## Enzymatic conversion of carbon dioxide†

Jiafu Shi,<sup>‡,abc</sup> Yanjun Jiang,<sup>‡,d</sup> Zhongyi Jiang,<sup>\*,ac</sup> Xueyan Wang,<sup>ac</sup> Xiaoli Wang,<sup>ac</sup> Shaohua Zhang,<sup>ac</sup> Pingping Han<sup>ac</sup> and Chen Yang<sup>ac</sup>

With the continuous increase in fossil fuels consumption and the rapid growth of atmospheric CO<sub>2</sub> concentration, the harmonious state between human and nature faces severe challenges. Exploring green and sustainable energy resources and devising efficient methods for CO<sub>2</sub> capture, sequestration and utilization are urgently required. Converting CO<sub>2</sub> into fuels/chemicals/materials as an indispensable element for CO<sub>2</sub> capture, sequestration and utilization may offer a win-win strategy to both decrease the CO<sub>2</sub> concentration and achieve the efficient exploitation of carbon resources. Among the current major methods (including chemical, photochemical, electrochemical and enzymatic methods), the enzymatic method, which is inspired by the CO<sub>2</sub> metabolic process in cells, offers a green and potent alternative for efficient CO<sub>2</sub> conversion due to its superior stereo-specificity and region/chemo-selectivity. Thus, in this tutorial review, we firstly provide a brief background about enzymatic conversion for CO<sub>2</sub> capture, sequestration and utilization. Next, we depict six major routes of the CO<sub>2</sub> metabolic process in cells, which are taken as the inspiration source for the construction of enzymatic systems *in vitro*. Next, we focus on the state-of-the-art routes for the catalytic conversion of CO<sub>2</sub> by a single enzyme system and by a multienzyme system. Some emerging approaches and materials utilized for constructing single-enzyme/multienzyme systems to enhance the catalytic activity/stability will be highlighted. Finally, a summary about the current advances and the future perspectives of the enzymatic conversion of CO<sub>2</sub> will be presented.

Received 28th February 2015

DOI: 10.1039/c5cs00182j

[www.rsc.org/chemscrev](http://www.rsc.org/chemscrev)

### Key learning points

1. Major routes of enzymatic conversion of CO<sub>2</sub> in cells.
2. Reaction processes/mechanisms of CO<sub>2</sub> conversion catalyzed by a single enzyme (oxidoreductases or lyases).
3. Reaction processes/mechanisms of CO<sub>2</sub> conversion catalyzed by multiple enzymes.
4. Strategies for designing and constructing enzyme catalysis systems with high activity and stability.
5. Future outlook and perspectives on the enzymatic conversion of CO<sub>2</sub>.

## 1. Introduction

Carbon capture, sequestration and utilization (CCSU) has been widely recognized as an efficient option for reducing atmospheric CO<sub>2</sub> concentration. In general, CO<sub>2</sub> capture can be regarded as

the process of capturing waste CO<sub>2</sub> from specific sources, such as fossil-fuel power plants; CO<sub>2</sub> sequestration can be regarded as the process of transporting/depositing enriched CO<sub>2</sub> to a storage site (mineralization or landfill); and CO<sub>2</sub> utilization can be regarded as the process of directly using CO<sub>2</sub> as a reaction medium or transforming renewable CO<sub>2</sub> into useful chemicals, materials or fuels. For each process, some relatively mature technologies have been developed up to an industrial scale, such as the alkaline absorption process (for CO<sub>2</sub> capture), mineralization process, landfill process (for CO<sub>2</sub> sequestration), supercritical CO<sub>2</sub> extraction process, urea synthesis process, methanol synthesis process, carboxylation of phenols, carboxylation of epoxides and the carboxylation of pyrrole (for CO<sub>2</sub> utilization). Numerous bench-scale or industrial-scale technologies have also been developed for enhancing the efficiency of CO<sub>2</sub> capture, sequestration and utilization. For most of the

<sup>a</sup> Key Laboratory for Green Chemical Technology of Ministry of Education, School of Chemical Engineering and Technology, Tianjin University, Tianjin 300072, China.  
E-mail: zhyjiang@tju.edu.cn

<sup>b</sup> School of Environmental Science and Engineering, Tianjin University, Tianjin 300072, China

<sup>c</sup> Collaborative Innovation Center of Chemical Science and Engineering (Tianjin), Tianjin, 300072, China

<sup>d</sup> School of Chemical Engineering and Technology, HeBei University of Technology, Tianjin 300130, China

† Electronic supplementary information (ESI) available. See DOI: 10.1039/c5cs00182j

‡ JF Shi and YJ Jiang contributed equally.

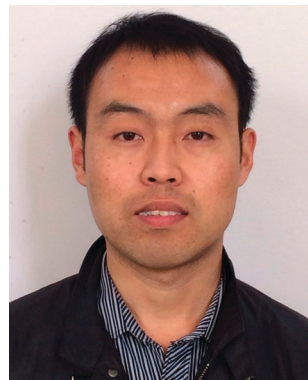
existing technologies, except for some physical processes (e.g., the landfill process and supercritical CO<sub>2</sub> extraction process), the CO<sub>2</sub> fixation/conversion reaction is undoubtedly a key and

common step.<sup>1–6</sup> So far, four major methods, including chemical, photochemical, electrochemical and enzymatic methods, have been exploited for catalyzing the CO<sub>2</sub> fixation/conversion reaction.



**Jiafu Shi**

*Jiafu Shi obtained a PhD in Chemical Engineering from Tianjin University in 2013 under the tutelage of Prof. Zhongyi Jiang. After graduation, he joined the faculty of Tianjin University, and started working at the School of Environmental Science and Engineering. His research interests include biocatalysis and hierarchically structured materials, which are related to environment. He has co-authored more than 40 SCI papers.*



**Yanjun Jiang**

*Yanjun Jiang obtained a PhD in Biochemical Engineering at the Tianjin University in 2009 under the tutelage of Prof. Zhongyi Jiang. He started working at School of Chemical Engineering and Technology, HeBei University of Technology, where he is currently an associate professor in biochemical engineering. His research interests include biocatalysis, biomass and bio-energy. He has co-authored more than 50 SCI papers, with a total citation time of over 400 and hindex of 14.*



**Zhongyi Jiang**

*Zhongyi Jiang is a professor at School of Chemical Engineering and Technology of Tianjin University. He obtained a PhD degree from Tianjin University in 1994. He was a visiting scholar of University of Minnesota with prof. Edward Cussler in 1997 and California Institute of Technology with prof. David Tirrell in 2009. He is the winner of National Science Fund for Distinguished Young Scholars in China. His research interest includes*

*biomimetic and bioinspired membranes and membrane processes, biocatalysis, photocatalysis. Till now, he has co-authored over 300 SCI papers, the total citation times is over 5000.*



**Xueyan Wang**

*Xueyan Wang received her bachelor degree in Bioengineering from Harbin University of Commerce in 2013. She is pursuing a MD under Associate Prof. Dong Yang at School of Chemical Engineering and Technology, Tianjin University. She is currently a MD student, whose research interest is biocatalysis.*



**Xiaoli Wang**

*Xiaoli Wang received her bachelor degree in Chemical Engineering and Technology from Xiamen University in 2010. She is pursuing a PhD under Prof. Zhongyi Jiang at School of Chemical Engineering and Technology, Tianjin University. She is currently a PhD student whose research interests include microcapsules, biomaterials and nanomaterials for biocatalysis applications.*



**Shaohua Zhang**

*Shaohua Zhang received his bachelor degree in Chemical Engineering and Technology from Tianjin University in 2013. He is now pursuing PhD degree under the tutelage of Prof. Zhongyi Jiang at the School of Chemical Engineering and Technology, Tianjin University. His research interests include biocatalysis, nanobiotechnology and nanostructured materials.*

In the first three methods, the selectivity is often low due to the abundant/stable form of the carbon element in the molecule of CO<sub>2</sub> and the difficulty in acquiring high-performance catalysts. The fourth method though, *i.e.*, the enzymatic method, may provide an eco-friendly and promising way for efficient CO<sub>2</sub> fixation/conversion because of its superior stereo-specificity and region/chemo-selectivity. Additionally, in the past decade, several excellent review papers about the catalytic conversion of CO<sub>2</sub> have been published, most of which focus on converting CO<sub>2</sub> through chemical or chemical-based methods.<sup>1–6</sup> Only one review paper offers an overview on the biosynthetic routes (*in vivo*) for CO<sub>2</sub>-fixation and a summary of detoxification processes (*in vitro*) catalyzed by lyases.<sup>1</sup> To the best of our knowledge, there is no review paper in the literature fully concerning the enzymatic conversion of CO<sub>2</sub> *in vitro*. Thus, in the following parts of this tutorial review, we will firstly give a summary of the CO<sub>2</sub> metabolic process in cells, in particular the CO<sub>2</sub> fixation/conversion reactions. The state-of-the-art reaction routes and mechanisms for the catalytic conversion of CO<sub>2</sub> by single enzyme system and by a multienzyme system (*in vitro*) will be subsequently depicted, with sporadic remarks included. Some emerging approaches and materials utilized for constructing single-enzyme/multienzyme systems to enhance the catalytic activity and stability will be briefly described. Finally, the bottleneck problems in the enzymatic conversion of CO<sub>2</sub>, as well as the future perspectives, will be presented.

## 2. Enzymatic conversion of CO<sub>2</sub> in cells

In nature, the fixation/conversion of CO<sub>2</sub> into organic material is a prerequisite for life and sets the starting point for biological evolution. In order to allow biological evolution to proceed efficiently, cells adopt six major routes (including the Calvin cycle, reductive citric acid cycle, reductive acetyl-CoA route, 3-hydroxypropionate cycle, 3-hydroxypropionate/4-hydroxybutyrate cycle and dicarboxylate/4-hydroxybutyrate cycle) for presenting the CO<sub>2</sub> metabolic process. In this section, these six major routes of the CO<sub>2</sub> metabolic process in cells will be illustrated (Fig. 1 and Table S1, specific information can also be found in Fig. S1–S6, ESI†) and discussed,<sup>7,8</sup> as they offer promising reaction routes for the conversion of CO<sub>2</sub> and the construction of enzymatic systems *in vitro*.

The Calvin cycle is one of the most important biosynthetic cycles on earth, and is used by the majority of photosynthetic organisms (such as plants, algae, cyanobacteria and most aerobic or facultative aerobic *Eubacteria*) to incorporate CO<sub>2</sub> into the cell carbon cycle (Fig. 1a). Thus, this cycle is, by far, the dominant method for CO<sub>2</sub> conversion in nature. In general, there are three stages and three key enzymes involved in the Calvin cycle. The three stages encompass CO<sub>2</sub> fixation (carboxylation,  $\Delta G^\circ < 0 \text{ kJ mol}^{-1}$  – note, specific data is unavailable), CO<sub>2</sub> reduction and the regeneration of the CO<sub>2</sub> receptor. In the first stage, 1,5-bisphosphate ribulose bisphosphate carboxylase (Rubisco) catalyzes the reaction between CO<sub>2</sub>

and 1,5-bisphosphate ribulose to form 3-phosphoglycerate (3 carbon compounds). Next, the 3-phosphoglycerate accepts a Pi from ATP to yield 1,3-diphosphoglycerate, and is further reduced to 3-phosphate glyceraldehyde by phosphoglyceraldehyde dehydrogenase. In the final stage, five-sixths of the acquired 3-phosphate glyceraldehyde transforms to 5-phosphate ribulose through a series of enzymatic reactions. Next, phosphoribulokinase activates 5-phosphate ribulose in an ATP-dependent condensation to produce 1,5-bisphosphate ribulose, which will be utilized as the CO<sub>2</sub> receptor to trigger the next cycle. Another one-sixth of the 3-phosphate glyceraldehyde will be converted into sugar, fatty acids, amino acids and so on.

The reductive citric acid cycle (also denoted as the reverse tricarboxylic acid cycle, the reverse TCA cycle or the reverse Krebs cycle) is basically the citric acid cycle run in reverse (Fig. 1b), which converts CO<sub>2</sub> and water into carbon compounds. This cycle was discovered in the anaerobic *Chlorobium limicola*, a green phototrophic sulfur bacterium, and is also seen in some thermophilic bacteria that grow on hydrogen, and certain bacteria that grow by reducing sulfate. The reductive citric acid cycle contains four carboxylation steps. First, succinyl-CoA is reductively carboxylated with CO<sub>2</sub> by  $\alpha$ -ketoglutarate synthase/2-oxoglutarate synthase (the first step,  $\Delta G^\circ +19 \text{ kJ mol}^{-1}$ ) to form  $\alpha$ -ketoglutarate/2-oxoglutarate at the expense of two equivalents of reduced ferredoxin. Next,  $\alpha$ -ketoglutarate/2-oxoglutarate and CO<sub>2</sub> are converted (the second step,  $\Delta G^\circ +8 \text{ kJ mol}^{-1}$ ) into isocitrate, catalyzed by isocitrate dehydrogenase at the expense of NADPH. Through a subsequent isomerism, isocitrate is converted into citrate, and then cleaved into oxaloacetate and acetyl-CoA by ATP citrate lyase. The latter compound is carboxylated with CO<sub>2</sub>, which requires the key enzyme pyruvate synthase (the third step,  $\Delta G^\circ +19 \text{ kJ mol}^{-1}$ ). The produced pyruvate is then activated by pyruvate kinase to yield phosphoenolpyruvate (PEP), followed by carboxylation with bicarbonate (the fourth step,  $\Delta G^\circ -24 \text{ kJ mol}^{-1}$ ). As a result, oxaloacetate is generated, and finally converted into succinyl-CoA by a series of enzymes.

The reductive acetyl-CoA route is mainly found in strictly acetogenic bacteria, acetogenic *Eubacteria* and methanogenic *Euryarchaeota*. This route was proposed in 1965 by Wood and Ljungdahl, and thus is also called the Wood–Ljungdahl route (Fig. 1c). Unlike the Calvin cycle and reductive citric acid cycle, the reductive acetyl-CoA route is a noncyclic route. Specifically, CO<sub>2</sub> is initially converted into formate by NADH-dependent formate dehydrogenase (F<sub>ate</sub>DH) ( $\Delta G^\circ +22 \text{ kJ mol}^{-1}$ ). Then, formate is captured by tetrahydrofolate and reduced into a methyl group, yielding methyl-H<sub>4</sub>folate. Methyltransferase (the corrinoid iron–sulfur protein) subsequently transfers the methyl group of methyl-H<sub>4</sub>folate to the cobalt center of the heterodimeric corrinoid iron–sulfur protein (Co<sup>I</sup>), thus acquiring the methylated corrinoid protein (CH<sub>3</sub>–Co<sup>III</sup>). Alternatively, CO dehydrogenase (CODH) functions to reduce CO<sub>2</sub> into CO ( $\Delta G^\circ 0 \text{ kJ mol}^{-1}$ ), while the acetyl-CoA synthase accepts the methyl group from CH<sub>3</sub>–Co<sup>III</sup> and converts CO, CoASH and the methyl group into acetyl-CoA.

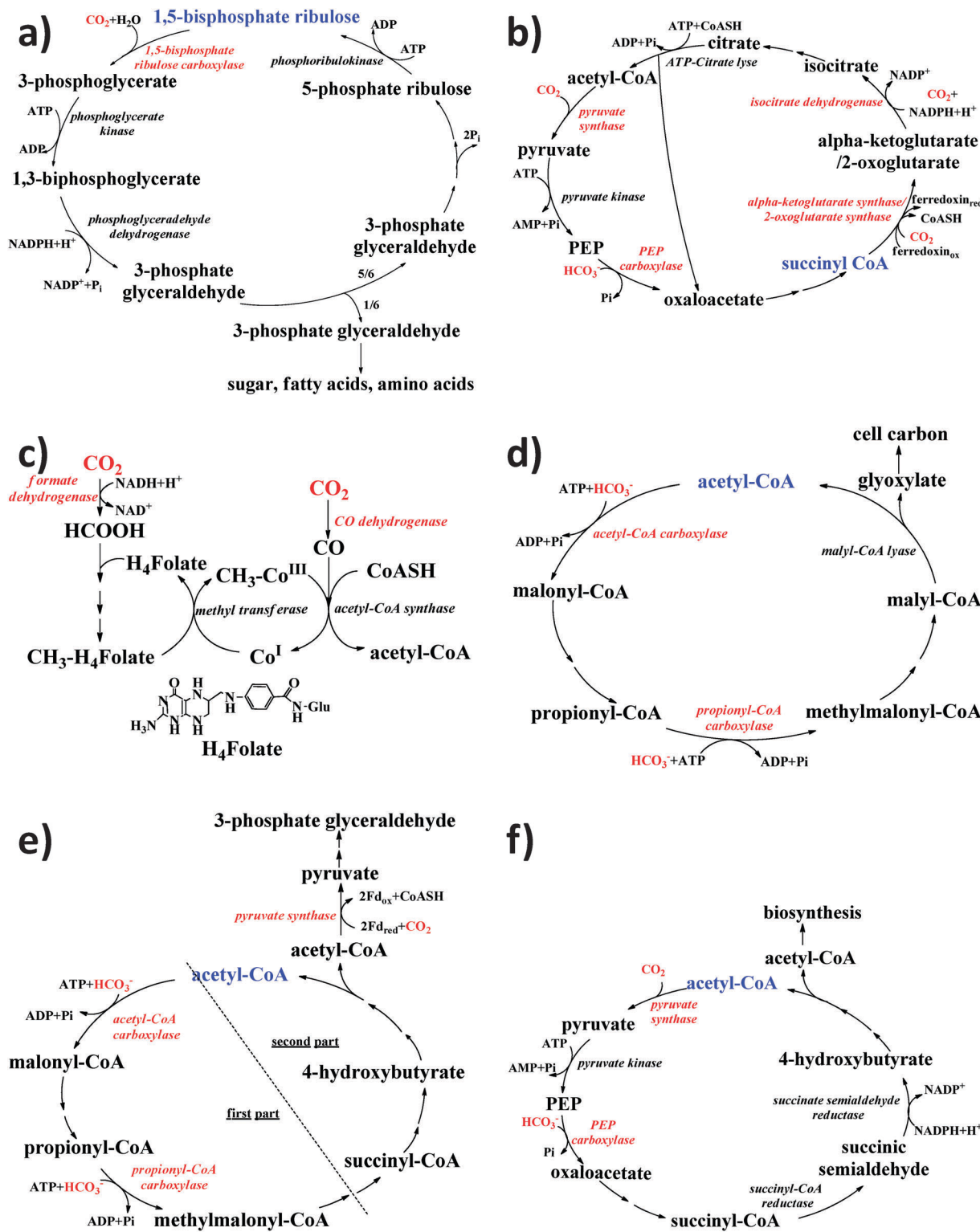


**Fig. 1** General illustration of the six major routes of the  $\text{CO}_2$  metabolic process in cells: (a) the Calvin cycle; (b) the reductive citric acid cycle; (c) the reductive acetyl-CoA route; (d) the 3-hydroxypropionate cycle; (e) the 3-hydroxypropionate/4-hydroxybutyrate cycle; and (f) the dicarboxylate/4-hydroxybutyrate cycle.  $\text{CO}_2$  (or bicarbonate) and the enzyme that directly catalyzes  $\text{CO}_2$  (or bicarbonate) are shown in red colour. The substrate/product in blue colour is the point where we start our descriptions of the cycle/route in the following parts. The standard free energy changes ( $\Delta G^\circ_f$  kJ mol<sup>-1</sup>, calculated from the standard free energies of formation at 25 °C) for the  $\text{CO}_2$  fixation/conversion steps are also added in the following description of the six cycles/routes.<sup>7,8</sup>

The 3-hydroxypropionate cycle was discovered in *Chloroflexaceae*, a facultatively aerobic, phototrophic bacterium (Fig. 1d).

In this cycle, two molecules of bicarbonate can be fixed. One molecule of bicarbonate is bound onto acetyl-CoA by acetyl-CoA

carboxylase in the presence of ATP, thus yielding malonyl-CoA ( $\Delta G^\circ = -14 \text{ kJ mol}^{-1}$ ). After sequential reduction of the terminal carboxylate group, malonyl-CoA is converted into propionyl-CoA. The propionyl-CoA is then carboxylated with the other molecule of bicarbonate to yield methylmalonyl-CoA by the activation of the propionyl-CoA carboxylase ( $\Delta G^\circ = -11 \text{ kJ mol}^{-1}$ ). Through the following isomerization rearrangement and a series of redox reactions, methylmalonyl-CoA is converted into maryl-CoA, which is then split into acetyl-CoA and glyoxylate for replenishing the cycle and for further utilization in cells, respectively.

The 3-hydroxypropionate/4-hydroxybutyrate cycle is a relatively novel cycle found in *Metallosphaera*. The genes for this cycle also exist in other archaea that are either microaerophiles or strict anaerobes. As shown in Fig. 1e, this cycle can be divided into two parts with three key enzymes, including acetyl-CoA carboxylase, propionyl-CoA carboxylase and pyruvate synthase. In the first part, acetyl-CoA carboxylase activates acetyl-CoA in an ATP-dependent condensation with bicarbonate, thus yielding malonyl-CoA ( $\Delta G^\circ = -14 \text{ kJ mol}^{-1}$ ). Through a five-enzyme cascade reaction, propionyl-CoA is synthesized from malonyl-CoA. Then, this propionyl-CoA is converted into methylmalonyl-CoA by propionyl-CoA carboxylase in the presence of bicarbonate and ATP ( $\Delta G^\circ = -11 \text{ kJ mol}^{-1}$ ). After an isomerization rearrangement, methylmalonyl-CoA is quickly converted into succinyl-CoA. In the second part, succinyl-CoA is firstly reduced into 4-hydroxybutyrate, and then, one molecule of 4-hydroxybutyrate is converted into two molecules of acetyl-CoA after a series of cascade reactions with the participation of several enzymes. For these two molecules of acetyl-CoA, one assimilates CO<sub>2</sub> and is converted into 3-phosphate glyceraldehyde by pyruvate synthase ( $\Delta G^\circ = +19 \text{ kJ mol}^{-1}$ ), while the other is used to conduct the next cycle. Notably, this cycle has some similar/same intermediates as the 3-hydroxypropionate cycle, where succinyl-CoA is formed from acetate and two molecules of bicarbonate. After this point though, the two routes become different.

The dicarboxylate/4-hydroxybutyrate cycle mainly functions in the anaerobic autotrophic members of *Thermoproteales* and *Desulfurococcales*, which have adapted to a facultative aerobic energy metabolism at low oxygen pressure (Fig. 1f). This cycle starts from the reductive carboxylation of acetyl-CoA with CO<sub>2</sub> to generate pyruvate by pyruvate synthase ( $\Delta G^\circ = +19 \text{ kJ mol}^{-1}$ ). The produced pyruvate is then converted into PEP, followed by carboxylation with bicarbonate to acquire oxaloacetate ( $\Delta G^\circ = -12 \text{ kJ mol}^{-1}$ ). The subsequent reduction of oxaloacetate involves an incomplete reductive citric acid cycle that terminates at succinyl-CoA. The generated succinyl-CoA is further reduced into succinic semialdehyde and then into 4-hydroxybutyrate. Afterwards, one molecule of 4-hydroxybutyrate is converted into two molecules of acetyl-CoA via normal β-oxidation reactions. For the two molecules of acetyl-CoA, one is used for subsequent biosynthesis and the other serves as a CO<sub>2</sub> receptor for the next cycle.

As observed in the above-mentioned six major routes, the carbon source is either CO<sub>2</sub> or bicarbonate, which primarily depends on the specific “enzyme” in a specific CO<sub>2</sub> fixation/conversion reaction. Just owing to the difference in the carbon

source, a fast and effective (inter)conversion between CO<sub>2</sub> and bicarbonate is highly required. In this regard, nature has evolved an efficient enzyme – carbonic anhydrase (CA) – that can catalyze the (inter)conversion between CO<sub>2</sub> and bicarbonate in a fast and controllable manner in cells. As this enzyme and the (inter)conversion reaction are ubiquitous in cells (micro-organisms, plants, animals, etc.), corresponding information is not presented in Fig. 1.

Collectively, for all the six major routes of the CO<sub>2</sub> metabolic process in cells, the CO<sub>2</sub> fixation/conversion reaction is particularly important and, in which, oxidoreductases, synthases and lyases play crucial roles in accelerating the reaction rate and altering the reaction direction. To maintain the stability of such a complicated metabolic process, cells also create appropriate physicochemical microenvironments to suppress the denaturation of enzymes. Inspired by this, the conversion of CO<sub>2</sub> *in vitro* catalyzed by an enzyme extracted/screened from cells may provide a high-efficiency way to accomplish CO<sub>2</sub> capture, sequestration and utilization.

### 3. Conversion of CO<sub>2</sub> by a single enzyme *in vitro*

Directly adopting the single enzyme (oxidoreductases, synthases or lyases) that is in charge of accomplishing the CO<sub>2</sub> fixation/conversion reaction in cells to catalyze the conversion of CO<sub>2</sub> *in vitro* seems a feasible way to achieve CO<sub>2</sub> capture, sequestration and utilization. However, the reactions conducted by synthases (acetyl-CoA synthase, pyruvate synthase, acetyl-CoA carboxylase, etc.) usually involve CoA-containing substrates, and the acquired products are uncommon and often useless in our daily life, which make the synthases unsuitable for *in vitro* applications. Therefore, directly inspired from the six major routes, only two other classes of enzymes, namely oxidoreductases (*i.e.*, F<sub>ate</sub>DH, CO<sub>2</sub> reductase, CODH, remodeled nitrogenase, etc.) and lyases (*i.e.*, CA), have been discovered/extracted from specific organisms. Correspondingly, several kinds of fuels/chemicals/materials, including formate, CO, methane, bicarbonate, etc., have been successfully synthesized. This section will describe the state-of-the-art reaction routes for the catalytic conversion of CO<sub>2</sub> by a single enzyme. In addition, enlightened by the existing form and physicochemical environment of enzymes in cells, some advanced approaches and materials utilized for constructing enzymatic systems with enhanced catalytic activity and stability will also be described.

#### 3.1 Conversion of CO<sub>2</sub> by oxidoreductases

Theoretically, an oxidoreductase is a kind of enzyme that catalyzes the transferring of electrons from one molecule (the reductant or electron donor) to another (the oxidant or electron acceptor). During the redox reaction, NADPH/NADP<sup>+</sup> or NADH/NAD<sup>+</sup> is employed as an essential cofactor(s). The aim of converting CO<sub>2</sub> by an oxidoreductase is to reduce the oxidation state of the carbon element, and acquire carbon-based energy resources.

**3.1.1 Conversion of CO<sub>2</sub> to formate by formate dehydrogenase (F<sub>ate</sub>DH) or carbon dioxide (CO<sub>2</sub>) reductase.** The first choice of products from the conversion of CO<sub>2</sub> catalyzed by oxidoreductases should be formate or CO (eqn (1) and (2)). Undoubtedly, CO is an important chemical and fuel. Alternatively, formate is also an important chemical as it can be utilized for methanol production, hydrogen production, direct formic acid fuel cells, etc.



As mentioned in the third route of the CO<sub>2</sub> metabolic process (the reductive acetyl-CoA route), CO<sub>2</sub> could be fixed and converted into formate *in vivo* catalyzed by F<sub>ate</sub>DH (a typical oxidoreductase) with NADH as a cofactor. The mechanism for the reduction of CO<sub>2</sub> to formate by this NADH-dependent F<sub>ate</sub>DH can be simply proposed as the direct transferring of hydride from the C<sub>4</sub> atom of the pyridine ring in NADH to the C atom of CO<sub>2</sub> (Fig. 2). CO<sub>2</sub> and NADH are positioned in close proximity to facilitate the hydride transferring. After the generation of formate, NAD<sup>+</sup> with a bipolar conformation is left.<sup>9</sup> Intrigued by this route, several research groups (such as Baeg's group, Amao's group, Müller's group, Hirst's group, Jiang's group)<sup>10–16</sup> have utilized NADH-dependent F<sub>ate</sub>DH to convert CO<sub>2</sub> and have systematically investigated the catalytic performance. In order to acquire high stability (especially recycling stability) of the enzymes, Jiang and co-workers<sup>15</sup> encapsulated NADH-dependent F<sub>ate</sub>DH from *Candida boidinii* into a series of millimetre-sized sol-gel carriers, including silica gels, alginate-silica gels, hydroxyapatite-polysaccharide gels, etc. Once applied for reducing CO<sub>2</sub> at the expense of NADH, the immobilized enzymes exhibited desirable activity and high stability (the formate yield could reach as high as *ca.* 95.6% for a 8 h reaction), primarily because the suitable structures of the

carriers offered favourable microenvironments to preserve the 3-D structure of the enzymes. Unfortunately, in the above case, the cofactor in either the free or immobilized systems was a sacrificial reagent. Considering its high cost, coupling of the enzymatic conversion of CO<sub>2</sub> and the cofactor regeneration was urgently required.

To achieve this goal, an artificial photosynthesis system was established through coupling the graphene-based photocatalyst and NADH-dependent F<sub>ate</sub>DH by Baeg and co-workers.<sup>12</sup> The resulting photosynthesis system (CCGCMAQSP) was mainly composed of the chemically converted graphene (CCG), the chromophore covalently bound with CCG (multianthraquinone-substituted porphyrin, MAQSP) and a kind of enzyme (NADH-dependent F<sub>ate</sub>DH) in free form. The mechanism of this photosynthetic process is illustrated in Fig. 3. Specifically, the absorption of the photon firstly occurred as a transition between localized orbitals around the chromophore (MAQSP). The generated electrons then transferred and reached the rhodium complex *via* the graphene surface. After accepting the electrons, the rhodium complex was reduced. The reduced rhodium complex then extracted a proton from the bulk aqueous solution, and transferred the electrons and a hydride to NAD<sup>+</sup> for NADH regeneration. Then, the regenerated NADH was consumed during the CO<sub>2</sub>-to-formate conversion process, and finally the whole regeneration cycle was accomplished. Baeg and co-workers<sup>12</sup> also constructed two other kinds of artificial photosynthesis systems through coupling W<sub>2</sub>Fe<sub>4</sub>Ta<sub>2</sub>O<sub>17</sub> and MAQSP photocatalysts with NADH-dependent F<sub>ate</sub>DH. In Fig. 3b and c, the investigations of NADH regeneration and formate production clearly reveal the superiority of the CCGCMAQSP-based artificial photosynthesis system over the two other systems. Based on the previous exploitations, Amao and co-workers<sup>11</sup> also constructed an immobilized artificial leaf device through co-immobilizing chlorin-e6 (as a photosensitised dye), a viologen with a long alkyl chain (as an electron donor) and

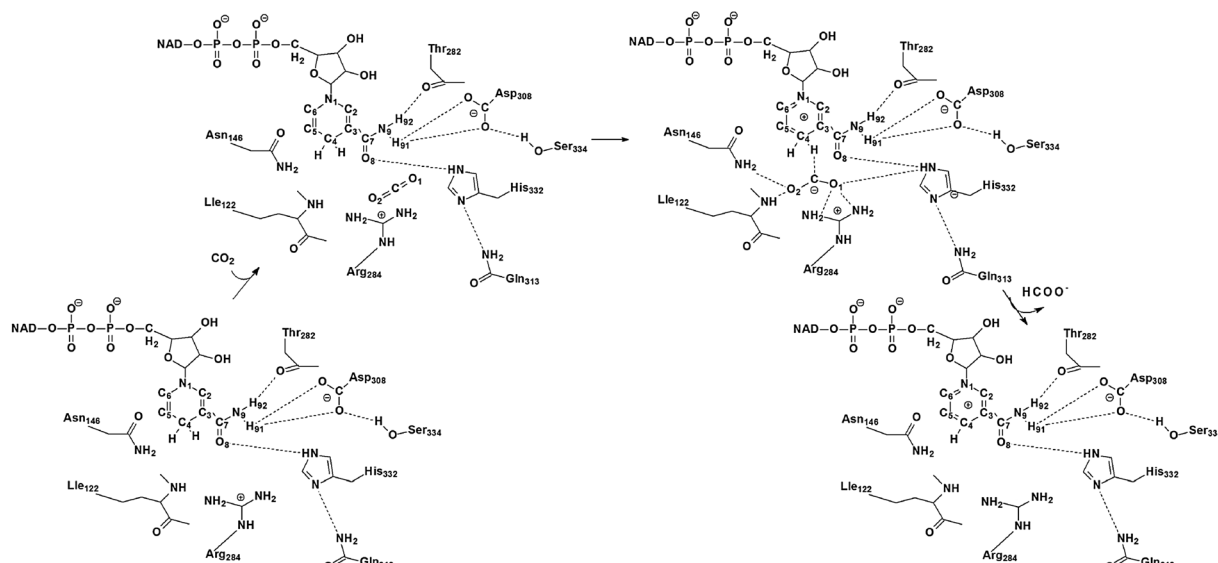
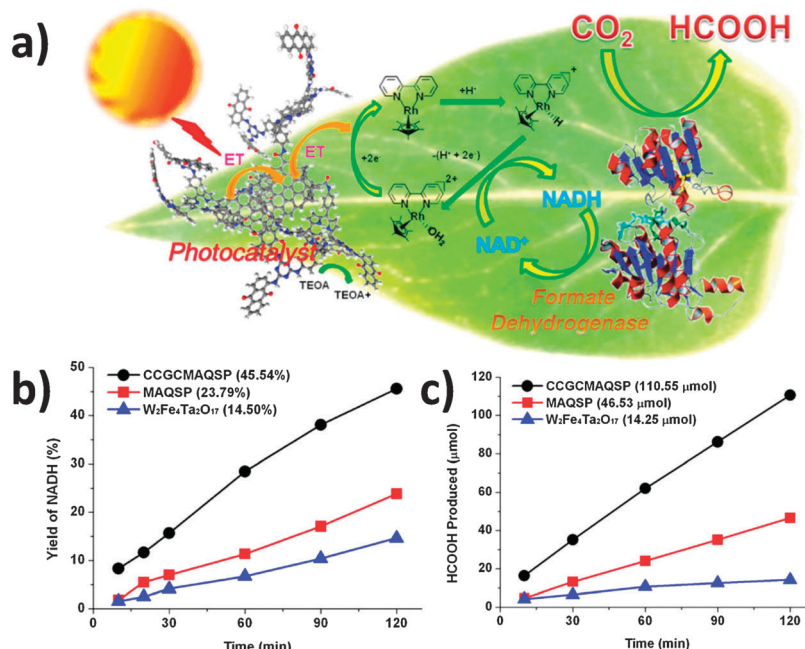


Fig. 2 The mechanism for the reduction of CO<sub>2</sub> to formate by NADH-dependent F<sub>ate</sub>DH.<sup>9</sup>



**Fig. 3** (a) Artificial photosynthesis of formate from CO<sub>2</sub> catalyzed by the photocatalyst-enzyme coupled system under visible light; and (b) time dependence of the NADH yield and (c) formate production using the photocatalyst-enzyme coupled system under visible light irradiation. Reproduced with permission from ref. 12. Copyright 2012 American Chemistry Society.

NAD(P)H-dependent F<sub>ate</sub>DH from *Saccharomyces cerevisiae* on a silica gel-based substrate for catalytically converting CO<sub>2</sub>. When the CO<sub>2</sub>-saturated NAD(P)H aqueous solution (the cofactor) flowed onto the artificial leaf device under visible light irradiation, the formate concentration increased with the prolongation of the irradiation time, indicating the essential role that solar energy plays in the production of formate from CO<sub>2</sub>. More importantly, this artificial leaf device could enhance the enzyme stability and regenerate the cofactor simultaneously.

Previous studies indicated that the ion-type cofactor, mainly referring to NADH, was required in the catalytic reduction of CO<sub>2</sub> to formate when adopting NADH-dependent F<sub>ate</sub>DH as the catalyst. However, the high cost and difficult availability of an ion-type cofactor may restrict further applications of this enzymatic route. Very recently though, a great breakthrough was reported by Müller and co-workers.<sup>10,14</sup> They discovered a bacterial hydrogen-dependent CO<sub>2</sub> reductase (HDCR, from the acetogenic bacterium *Acetobacterium woodii*) that could directly use H<sub>2</sub> as a “cofactor” for converting CO<sub>2</sub> into formate. The HDCR enzyme was composed of four different subunits (Fig. 4), including a putative formate dehydrogenase (FdhF1/2) and an iron–iron hydrogenase (HydA2) as the two large subunits neighboured by two small electron transfer subunits (HycB2/3). Amongst these, FdhF1/2 acted as the catalyst for reducing CO<sub>2</sub> into formate, while HydA2 was in charge of activating/oxidizing H<sub>2</sub> into two H<sup>+</sup> accompanied with acquiring two electrons and HycB2/3 was responsible for transferring the two electrons from HydA2 to FdhF1/2. Once utilized for the catalytic conversion of CO<sub>2</sub> and H<sub>2</sub> to formate, the reaction rate was as high as 10 mmol min<sup>-1</sup> mg<sup>-1</sup>. The TOF was calculated to be 101 600 h<sup>-1</sup>, which is nearly 1500 times higher than that of

chemical catalysis ( $\sim 70\text{ h}^{-1}$ ). One remarkable advantage of this route should be the independence of the external ion-type cofactor. Moreover, as illustrated in Fig. 4, the HDCR can also catalyze the reduction of CO<sub>2</sub> with reduced ferredoxin as a “cofactor”. As ferredoxin can be reduced by CO dehydrogenase (CODH) from *Acetobacterium woodii*, formate can also be produced from CO once the HDCR, CODH and ferredoxin are integrated into one system. Considering that industrially produced H<sub>2</sub> often contains a certain amount of CO, this

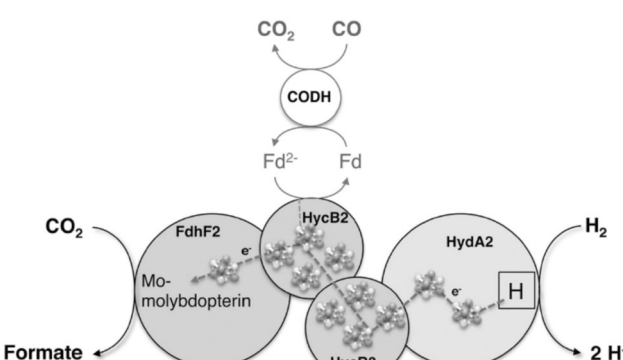


**Fig. 4** The model of the hydrogen-dependent CO<sub>2</sub> reductase (HDCR) from *Acetobacterium woodii*. The electrons for CO<sub>2</sub> reduction are either provided by the hydrogenase subunit iron–iron hydrogenase (HydA2), where hydrogen oxidation takes place, or by the reduced ferredoxin. The latter can be reduced by using CO and CO dehydrogenase (CODH). The electrons are delivered to the active site for CO<sub>2</sub> reduction in selenium-containing formate dehydrogenase (FdhF2) via the electron-transferring subunits (HycB2/3). The iron sulfur clusters are shown in the central part of this figure.<sup>10,14</sup>

integrated system may allow the complete conversion of gas mixtures (or syngas) containing H<sub>2</sub>, CO<sub>2</sub> and CO.

Another breakthrough to address the issue of cofactor consumption/regeneration is finding the NADH-independent F<sub>ateDH</sub>, of which the active site is a molybdenum or tungsten center.<sup>6,13,17</sup> As a proposed mechanism for the reduction of CO<sub>2</sub> by this kind of F<sub>ateDH</sub>, two electrons are firstly transferred to the molybdenum or tungsten center, and then the Mo<sup>VI</sup> or W<sup>VI</sup> ion is reduced into the Mo<sup>IV</sup> or W<sup>IV</sup> ion. The reduced active site features a square pyramidal molybdenum or tungsten center that is coordinated to four sulfur atoms from two pyranopterin ligands in the basal plane and a fifth sulfur atom in an apical position. The selenocysteine ligand is simultaneously released from the active site. Afterwards, one H<sup>+</sup> ion is transferred to the N atom of the imidazole ring to form an intermediate that is utilized as a proton donor in the subsequent step. Once CO<sub>2</sub> is contacted with the active site, a C-H bond is formed and a C=O bond is cleaved into a C-O bond. Accordingly, formate is formed. During the formation process of the C-H bond, the arginine residue assists in orienting the formate ligand for the proton removal/delivery by the histidine residue. Obviously, different from the hydride transfer mechanism of

the NADH-dependent F<sub>ateDH</sub>, the molybdenum- or tungsten-containing enzymes transfer the two electrons and the H<sup>+</sup>/proton to different sites. Based on this finding, Hirst and co-workers utilized both molybdenum- and tungsten-containing F<sub>ateDH</sub> to convert CO<sub>2</sub> into formate.<sup>13,17</sup> Taking tungsten-containing F<sub>ateDH</sub> as an example, they directly adsorbed F<sub>ateDH</sub> from *S. fumaroxidans* on an electrode surface, which exhibited high efficiency in the catalytic reduction of CO<sub>2</sub> to formate. Briefly, as shown in Fig. 5a, two electrons were transferred from the electrode to the active site (buried inside the insulating protein interior) by the iron-sulfur clusters, thus reducing CO<sub>2</sub> into formate through forming a C-H bond and cleaving a C=O bond. As illustrated in Fig. 5b, the rate for this reaction was highly sensitive to the pH value, which was found to increase sixfold from pH 7.5 to 5.5. The highest current density corresponded to an average turnover frequency of 112 s<sup>-1</sup> from a monolayer of tungsten-containing F<sub>ateDH</sub>. This value is about two orders of magnitude faster than CO<sub>2</sub> hydrogenation by ruthenium complexes in supercritical CO<sub>2</sub> and 10 times faster than photosynthetic CO<sub>2</sub> activation during the carboxylation of 1,5-bisphosphate ribulose by Rubisco. Notably, in Hirst's work, the oxidation of formate was also conducted by using

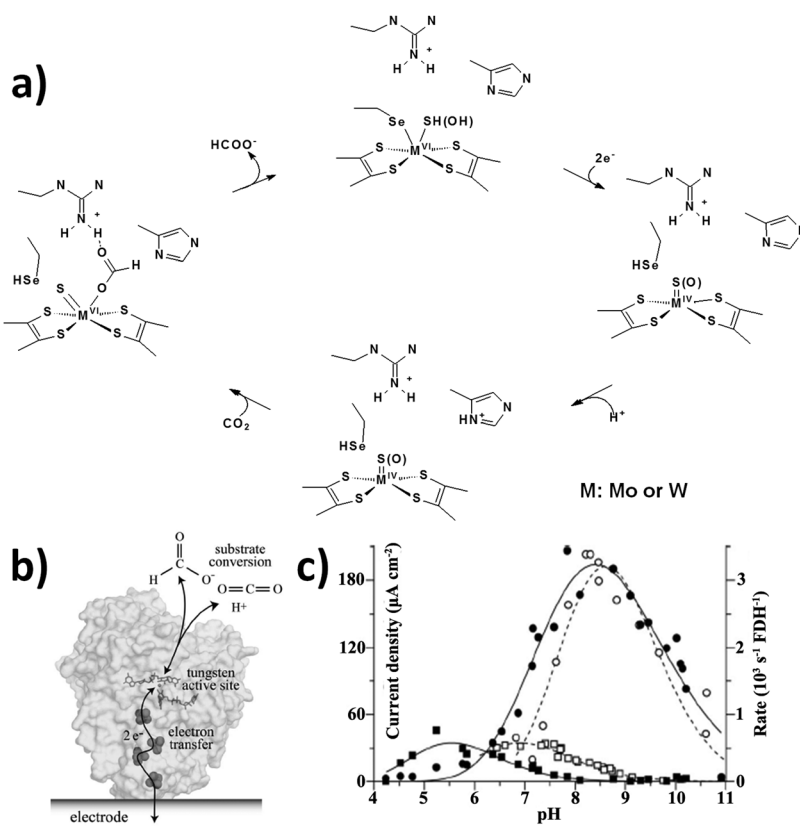


Fig. 5 (a) The proposed mechanism for the reduction of CO<sub>2</sub> to formate by molybdenum- or tungsten- containing F<sub>ateDH</sub>;<sup>6,17</sup> (b) the schematic of the catalytic (inter)conversion between CO<sub>2</sub> and formate by F<sub>ateDH</sub> adsorbed on an electrode surface (herein, the structure shown in (a) is that of the tungsten-containing F<sub>ateDH</sub> from *Desulfovibrio gigas*); (c) the kinetics of this catalytic reaction by tungsten-containing F<sub>ateDH</sub> as a function of pH value. Current densities from the first voltammetric scan in 10 mM formate and 10 mM CO<sub>2</sub> at 0.25 V overpotential are compared to data from conventional assays in solution in 10 mM formate or 10 mM CO<sub>2</sub>. (Open square, rate of CO<sub>2</sub> reduction in solution; filled square, rate of catalytic reduction of CO<sub>2</sub>; open circle, rate of formate oxidation in solution; filled circle, rate of catalytic oxidation of formate.) Reproduced with permission from ref. 13. Copyright 2012 National Academy of Sciences, United States.

this system (Fig. 5b). However, no corresponding discussion is given on this in our tutorial review owing to its weak relevance to our main topic.

**3.1.2 Conversion of CO<sub>2</sub> to carbon monoxide (CO) by carbon monodioxide dehydrogenase (CODH).** CO, another important product from the reduction of CO<sub>2</sub>, is regarded as the key feedstock for various synthetic processes, such as the Fischer-Tropsch, Monsanto and Cativa processes. Meanwhile, CO also possesses significant fuel value and can be readily converted into methanol (as a liquid fuel). In nature, the (inter)conversion between CO and CO<sub>2</sub> is primarily catalyzed by [NiFe] CO dehydrogenases ([NiFe] CODH). As shown in Fig. 6a, the active site of [NiFe] CODH mainly consists of Ni and Fe centers bridged by a [3Fe–4S] cluster that positions these two metal centers in close proximity. The proposed mechanism for the reduction of CO<sub>2</sub> to CO by [NiFe] CODH is illustrated in Fig. 6b.<sup>6,18</sup> Generally, an overall two-electron process occurs during the whole reaction process: an electron transfer step to form the reduced Ni center, followed by a chemical step involving CO<sub>2</sub> bound to the reduced Ni center, and finally a second electron transfer step. For the chemical step, CO<sub>2</sub> binds to the Ni atom *via* the C atom to form a Ni–C bond. Simultaneously, one of the carboxylate oxygen atoms (O<sub>2</sub>) forms a hydrogen bond with a protonated histidine residue (H93). The loss of water from Fe<sub>1</sub> results in the formation of a CO<sub>2</sub> complex, in which another oxygen atom of the CO<sub>2</sub> molecule, O<sub>1</sub>, is bound to Fe<sub>1</sub> and forms a hydrogen bond with a protonated lysine residue (K563). Cleavage of the C–O<sub>1</sub> bond and the loss of water result in the formation of a Ni<sup>II</sup>CO species. This Ni<sup>II</sup>CO species readily releases CO and adds water to regenerate the starting Ni<sup>II</sup> complex and complete the catalytic cycle. Therefore, CO<sub>2</sub> binding, catalysis or even release in the enzyme appears to involve the activation by the two metal centers and additional stabilization from appropriately positioned residues in the second coordination sphere. Inspired by this *in vivo* enzymatic reaction, researchers have devoted tremendous effort to construct *in vitro* systems for converting CO<sub>2</sub> into CO efficiently.

The first report of utilizing [NiFe] CODH (from *Moorella thermoacetica*) to reduce CO<sub>2</sub> into CO *in vitro* was implemented by Shin and co-workers.<sup>19</sup> Since then, most of the representative studies in the last decades were accomplished by Armstrong and co-workers.<sup>20–24</sup> One of the significant advances in their investigations is the efficient combination of electrocatalysis/photocatalysis with the enzymatic conversion of CO<sub>2</sub> to CO. Traditionally, due to the highly uphill thermodynamics of one electron transferring to form CO<sub>2</sub><sup>•-</sup> ( $E = -1.9$  V vs. SHE in water, corrected to pH 7), the electrocatalytic/photocatalytic conversion of CO<sub>2</sub> usually requires a significant overpotential (hundreds of mV), which wastes a lot of energy. Moreover, this high-energy-input route may result in a mixture of products, including CO, methane and methanol. To address this issue, Armstrong and co-workers<sup>20</sup> immobilized [NiFe] CODH on a pyrolytic graphite “edge” (PGE) electrode, and systematically evaluated the activity of this enzyme rotating at high speed in an anaerobic sealed cell. In this process, the standard reduction potential for the (inter)conversion between CO<sub>2</sub> and CO catalyzed by [NiFe] CODH ( $E = -0.46$  V vs. SHE in water, at pH 6, or  $E = -0.51$  V vs. SHE in water, corrected to pH 7) was much higher than that without a catalyst ( $E = -1.9$  V vs. SHE in water, corrected to pH 7). This would then lead to a much lower required overpotential, along with an extremely high selectivity for yielding a specific product (CO, ~100%). Subsequently, they incorporated photocatalysis into the enzymatic conversion of CO<sub>2</sub> for constructing an artificial photosynthesis system.<sup>21,22</sup> Briefly, [NiFe] CODH as the catalyst and [RuII(bipy)<sub>2</sub>(4,4'-(PO<sub>3</sub>H<sub>2</sub>)<sub>2</sub>-bipy)]Br<sub>2</sub> (RuP; bipy = 2,2'-bipyridine) as the photosensitizer were both adsorbed on a series of n-type MOx semiconductor nanoparticles (*e.g.*, P25 TiO<sub>2</sub>, anatase TiO<sub>2</sub>, rutile TiO<sub>2</sub>, ZnO, SrTiO<sub>3</sub>, *etc.*) to construct a photocatalyst-enzyme coupled system. The principle of the CO<sub>2</sub> conversion process can be found in Fig. 7a. In detail, through the excitation with visible light, RuP injected electrons into the n-type MOx semiconductor conduction band (*e.g.*, -0.52 V for anatase TiO<sub>2</sub>, pH 6). These electrons then entered [NiFe] CODH through the D-cluster, and transferred through a second [Ni<sub>4</sub>Fe<sub>4</sub>S] cluster to

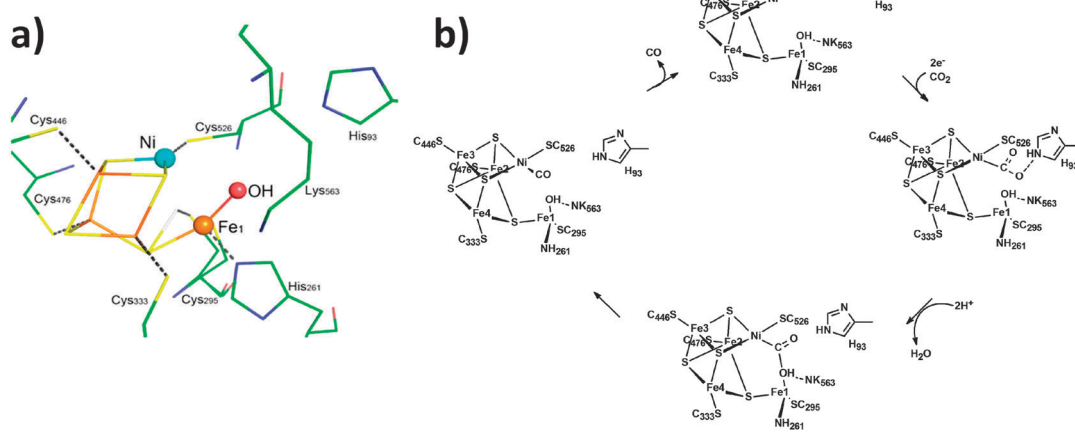
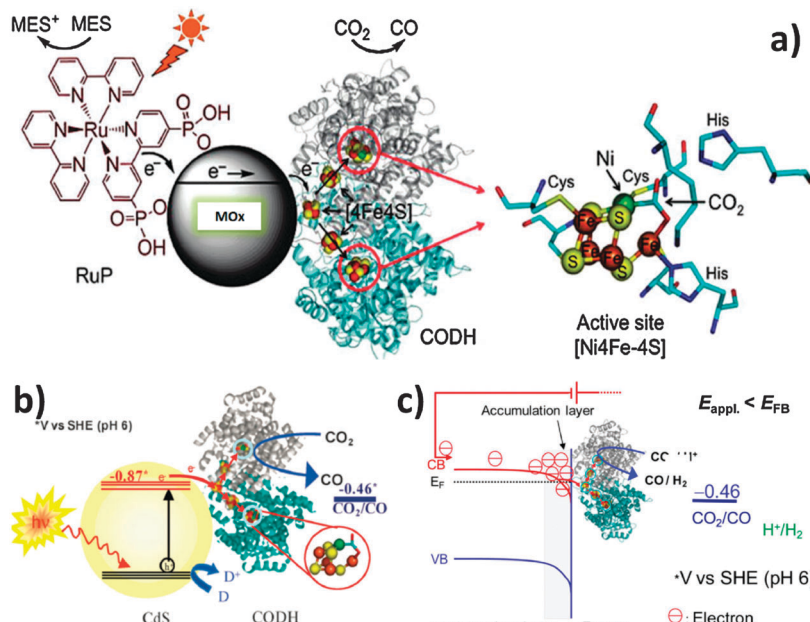


Fig. 6 (a) Ball-and-stick drawing of the active site of [NiFe] CODH and (b) the proposed mechanism for the reduction of CO<sub>2</sub> to CO by [NiFe] CODH.<sup>5,18</sup>



**Fig. 7** (a) Schematic of the  $\text{CO}_2$  photosynthesis system upon [NiFe] CODH attached to RuP-modified n-type metal oxide (MOx) semiconductors. A catalytic intermediate that is the active site in the enzyme [NiFe] CODH bound with  $\text{CO}_2$  is also shown (right in a). The oxidized photosensitizer is recovered by the sacrificial electron donor. Reprinted with permission from ref. 21. Copyright 2010 American Chemistry Society; (b) schematic of visible light-driven  $\text{CO}_2$  reduction upon [NiFe] CODH-CdS nanocrystal assemblies in the presence of an electron donor. Reprinted with permission from ref. 23. Copyright 2012 Royal Society of Chemistry; and (c) schematic of the formation of an electron accumulation layer at the surface of CdS or MOx when the applied electrode potential is lowered to the flatband potential ( $E_{\text{FB}}$ ). The increased electron density and subsequent downward band bending facilitate efficient electron transferring to the enzyme active site via [Ni4Fe4S] clusters to reduce  $\text{CO}_2$ . Reprinted with permission from ref. 24. Copyright 2013 American Chemistry Society.

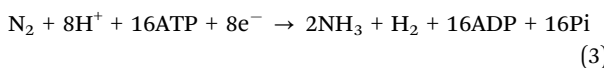
the active site, where  $\text{CO}_2$  was reduced into CO. Through an oxidation process, the photosensitive dye could be regenerated by a sacrificial electron donor (e.g., (2-(*N*-morpholino)ethane-sulfonic acid (MES), etc.). After carefully manipulating the factors (including coverage of the enzyme and RuP on the n-type MOx semiconductor nanoparticles, species of semiconductors, species of electron donors, etc.), the photosynthesis systems prepared with P25  $\text{TiO}_2$  and ordinary anatase  $\text{TiO}_2$  nanoparticles were confirmed to be the most effective catalysts, with an overall turnover frequency of  $0.14 \text{ s}^{-1}$ . This type of system is an excellent example for the further related investigations, although the turnover frequency was relatively lower than the expected result. Obviously, [NiFe] CODH, n-type MOx semiconductors, RuP and the sacrificial electron donor were essential in the above system. In particular, since most n-type MOx semiconductors possess a relatively wide band gap (such as  $\text{TiO}_2$ ,  $E_g = 3.1 \text{ eV}$ ), the semiconductors must be photosensitized by the co-attachment of a visible light harvesting RuP. The hole left on the RuP could then be quenched by a sacrificial electron donor. To simplify and intensify this process, Armstrong and co-workers<sup>23</sup> developed a Rub-free system, where [NiFe] CODH was assembled on CdS nanocrystals with visible-light harvesting capability (the conduction band (CB) edge of bulk CdS was at  $E_{\text{CB}} = -0.87 \text{ V vs. SHE}$  in water, at pH 6), which offered sufficient driving force to reduce  $\text{CO}_2$  into CO (reduction potential  $-0.46 \text{ V vs. SHE}$  in water, at pH 6) (Fig. 7b). After assaying the activity of reducing  $\text{CO}_2$  into CO under visible light

through tailoring the sacrificial agents and particle size/shape (CdS nanocrystal), the average turnover frequency for the [NiFe] CODH-CdS<sub>nanorods</sub> assemblies could be as high as  $1.23 \text{ s}^{-1}$ . This value was much higher than that reported by using supramolecular or semiconductor photocatalysts ( $< 0.14 \text{ s}^{-1}$ ). Very recently, the mechanism for the light-harvesting n-type semiconductors altering the bias of the reversible catalysts ([NiFe] CODH) in favour of  $\text{CO}_2$  reduction was clarified by Armstrong's and Nørskov's groups.<sup>24,25</sup> Similar conclusions were derived and summarized as follows. On the basis of the previously established models,<sup>24,25</sup> the surface electron concentration increased exponentially as the potential was lowered, and could be controlled by the difference between the flatband potential ( $E_{\text{FB}}$ ) and the applied electrode potential. When the applied electrode potential was lower than  $E_{\text{FB}}$ , a transformation to a metallic-like character occurred as an accumulation layer formed (Fig. 7c). Therefore, the increase in electron density at the semiconductor-enzyme interface favoured the efficient electron transferring from the n-type semiconductor to the enzyme for driving the reduction process. This principle or mechanism offers a further design criterion for artificial chemical/energy conversion systems.

Besides the [NiFe] CODH enzyme that can directly convert  $\text{CO}_2$  into CO, other types of oxidoreductases in nature may also render the possibility of catalyzing this reduction. Fortunately, Seefeldt and co-workers<sup>26</sup> found that nitrogenase from *Azotobacter vinelandii*, a kind of enzyme that commonly catalyzes the

six-electron reduction of  $\text{N}_2$  to ammonia, could catalyze the two-electron reduction of  $\text{CO}_2$ . To verify this possibility, CO acquired from the reduction of  $\text{CO}_2$  was quantified by using nitrogenase as the catalyst. A time-dependent production of CO was found, providing strong evidence for the reduction of  $\text{CO}_2$  to CO catalyzed by nitrogenase. This finding should expand the routes available for reducing  $\text{CO}_2$  into CO by seeking enzymes in a much broader range.

**3.1.3 Conversion of  $\text{CO}_2$  to methane catalyzed by remodeled nitrogenase.** As illustrated in the final part of section “3.1.2 Conversion of  $\text{CO}_2$  to carbon monoxide (CO) by carbon monooxide dehydrogenase (CODH)”, nitrogenase might also be able to catalyze the two-electron reduction of  $\text{CO}_2$  to yield CO since it can effectively catalyze the multielectron (six-electron) reduction of  $\text{N}_2$ . Fortunately, the feasibility of this reaction has been demonstrated by Seefeldt and co-workers.<sup>26</sup> At the beginning of their investigation, Seefeldt and co-workers wondered whether this nitrogenase could catalyze the eight-electron reduction of  $\text{CO}_2$  to the level of methane. Unfortunately, when the wild-type (or native) nitrogenase was employed for reducing  $\text{CO}_2$ , no methane was detected over a 20 min-reaction (Fig. 8b), indicating that native nitrogenase cannot trigger this reaction. Since several amino acids ( $\alpha$ -195,  $\alpha$ -70,  $\alpha$ -191, etc.) that approach the FeMo-cofactor (the active site, Fig. 8a) in nitrogenase play quite an important role in controlling substrate binding and in the reduction, then substitution of these amino acids with appropriate molecules may alter the catalytic behavior. To their surprise, they found that by remodeling the nitrogenase by substituting the  $\alpha$ -195 by Gln and  $\alpha$ -70 by Ala, they were able to catalyze the formation of methane from  $\text{CO}_2$ , forming up to 16 nmol (methane) nmol<sup>-1</sup> (MoFe protein) over a 20 min-reaction (Fig. 8b). The reaction rate mainly depended on the partial pressure of  $\text{CO}_2$  (or bicarbonate concentration) and the electron flux through the remodeled nitrogenase.



The mechanism for the reduction of  $\text{CO}_2$  by the remodeled nitrogenase is similar to that of  $\text{N}_2$  reduction by the native nitrogenase (eqn (3)).<sup>27</sup> As reported, metal-bound hydrides were an integral part of the FeMo-cofactor for activating  $\text{N}_2$ , which was considered to participate in the initial reduction of  $\text{N}_2$  to the intermediate diazene ( $\text{HN}=\text{NH}$ ). Further reduction of the metal-bound diazene into two ammonia molecules was proposed after the successive addition of electrons and protons. No detection of the proposed reaction intermediates (diazene  $\text{HN}=\text{NH}$  or hydrazine  $\text{H}_2\text{N}-\text{NH}_2$ ) suggested that the intermediates were bound to the active site until the final products were formed and released. This phenomenon could be explained by the stabilization of the key intermediates through appropriate functional groups, thus minimizing the kinetic barriers of this reaction. Similarly, the remodeled nitrogenase might also stabilize the key intermediates through appropriate functional groups in the multielectron reduction of  $\text{CO}_2$  to methane (eqn (4)). Specifically, metal-bound hydrides may participate in the initial steps in the  $\text{CO}_2$  reduction. The possible reaction occurring in this step should be the two-electron reduction of  $\text{CO}_2$  by hydride insertion. Further reduction of the metal-bound intermediates (e.g., metal-bound formate or metal-bound formaldehyde) into methane could be continued once sufficient electrons and protons were successively supplied. Besides the route of  $\text{CO}_2$  to methane, remodeled nitrogenase can also catalyze the coupling of  $\text{CO}_2$  with acetylene, yielding predominately propylene. Collectively, the finding described in this section provides insights into the broader context of how  $\text{N}_2$  is reduced to ammonia by enzymes. Future studies should focus on lowering the reaction barriers through stabilizing the key reaction intermediates in order to reduce  $\text{CO}_2$  into a larger variety of hydrocarbons.

### 3.2 Conversion of $\text{CO}_2$ by lyases

A lyase is an enzyme that catalyzes the breaking of chemical bonds rather than by hydrolysis or oxidation, and then generates a new double bond or a new ring structure. The reverse reaction (called “Michael addition”) catalyzed by a lyase

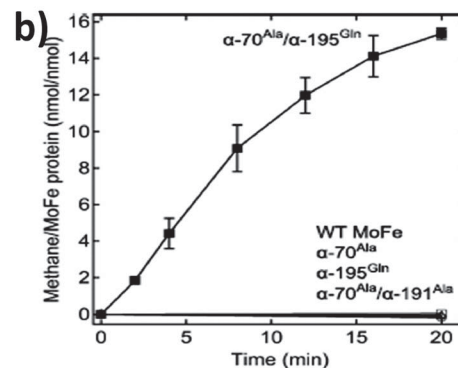
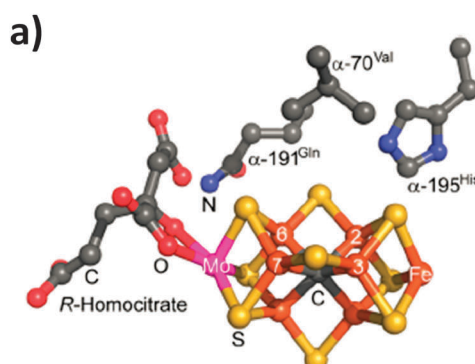


Fig. 8 (a) The FeMo-cofactor with some key amino acid residues (colors: Mo, magenta; Fe, rust; S, yellow; C, gray; O, red; N, blue); and (b) the methane formation as a function of time for different MoFe proteins.  $\text{CO}_2$  reduction to methane is shown as a function of time for the wild-type (or native) (○),  $\alpha$ -70Ala (◊),  $\alpha$ -195Gln (△),  $\alpha$ -70Ala/ $\alpha$ -191Ala (□), and  $\alpha$ -70Ala/ $\alpha$ -195Gln (■) MoFe proteins. Reprinted with permission from ref. 27. Copyright 2012 National Academy of Sciences.

commonly exists in cells, which offers enlightenment into the carboxylation of raw molecules with  $\text{CO}_2$  to obtain valuable chemicals/materials.

### 3.2.1 Conversion of $\text{CO}_2$ to bicarbonate (or minerals) by carbonic anhydrase (CA).



Carbonic anhydrase (CA), as a typical lyase, commonly exists in nature (mammals, plants, algae and bacteria) and is mainly responsible for the (inter)conversion between  $\text{CO}_2$  and bicarbonate to maintain the acid–base balance in blood and other tissues (eqn (5)). CA is an archetypal example of convergent evolution, comprising at least five distinct classes of  $\alpha$ ,  $\beta$ ,  $\gamma$ ,  $\delta$  and  $\zeta$  with little structural similarity, but where all the CAs compose an active site of a divalent zinc ion or related metal ion. Taking  $[\text{Zn}]$  CA as an example, the proposed mechanism for the hydration of  $\text{CO}_2$  could be described as follows (Fig. 9):<sup>6,28</sup> The active sites of  $[\text{Zn}]$  CA can be considered as comprising a  $\text{Zn}^{2+}$  ion coordinated to three histidine residues and a water/hydroxide. The coordination of water increases its acidity to a  $\text{pK}_a$  value of approximately 7, which allows the coordinated water to be deprotonated with weak bases to produce a hydroxide ligand. This hydroxide can then undergo a nucleophilic attack at the C atom of  $\text{CO}_2$  to yield a bicarbonate molecule stabilized by hydrogen bonding to a Thr residue and other residues in the second coordination sphere. A hydrophobic pocket formed by three Val residues assists in the positioning of  $\text{CO}_2$  for the nucleophilic attack by the hydroxide ligand. The displacement of bicarbonate by water could then regenerate the catalyst. Key features of this mechanism are the activation of water by binding to  $\text{Zn}^{2+}$ , the precise positioning of  $\text{CO}_2$  in a hydrophobic pocket and hydrogen bonding sites positioned in the second coordination sphere of Zn. Besides, the turnover frequency of  $[\text{Zn}]$  CA can be as high as  $\sim 10^6 \text{ s}^{-1}$ , making  $[\text{Zn}]$  CA one of the most efficient enzymes in nature. Just owing to the extremely high catalytic efficiency, CA has displayed great potential in  $\text{CO}_2$  capture and sequestration.

To the best of our knowledge, the CA-catalytic conversion of  $\text{CO}_2$  has so far been applied for assisting three techniques (absorption, membrane separation and precipitation/mineralization) during  $\text{CO}_2$  capture, sequestration and utilization.<sup>2</sup> One of the most successful cases involved the incorporation of the CA-catalytic conversion of  $\text{CO}_2$  into the chemical absorption of  $\text{CO}_2$  with regenerable alkaline aqueous solvents. In a traditional chemical absorption process,  $\text{CO}_2$  was removed from the mixing gas (this mainly refers to flue gas) in the absorber column and then desorbed in a heated stripper column to obtain relatively pure  $\text{CO}_2$ . In this process, the major challenge was that, as the alkaline aqueous solvents bond  $\text{CO}_2$  so tightly, the parasitic energy loss in desorbing  $\text{CO}_2$  could double the cost of electricity. The combination of a CA-catalytic conversion process and chemical absorption process could both increase the absorption rate of  $\text{CO}_2$  in the alkaline aqueous solvents and facilitate the use of aqueous solvents with a lower heat/energy input for desorption (Fig. 10). However, the relatively harsh conditions in the absorption processes (*i.e.*, temperatures of 50–125 °C; high concentrations of organic amines; trace contaminants) can cause the denaturation of the enzyme and reduce the enzyme activity/stability. To overcome this limitation, several approaches have been developed, including sourcing CA from thermophilic organisms, creating thermo-resistant CA by protein engineering techniques, immobilizing CA in/on suitable supports and by modifying the absorption process. As a very recent example, Lu and coworkers<sup>29</sup> developed a potassium carbonate-based absorption process for absorbing  $\text{CO}_2$  from coal combustion flue gas, where CA was used to accelerate the  $\text{CO}_2$  absorption process. To enhance the enzyme stability (including thermal/chemical resistance), CA was immobilized on nonporous silica-based nanoparticles. After conducting the absorption process in an alkaline solution over a 60 d period at 50 °C, the immobilized CA could retain 56–88% of its original activity, while only 30% of original activity was retained for the free CA. The second case involves the membrane separation technique assisted by the CA-catalytic conversion process, which was first

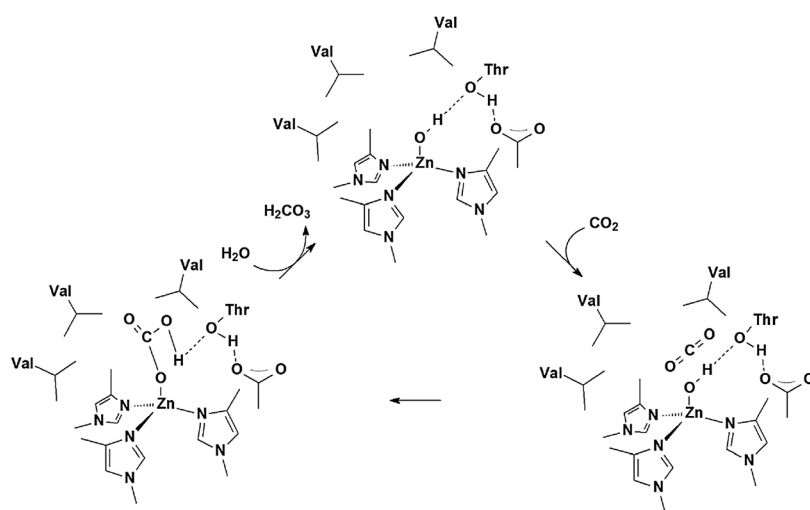


Fig. 9 Proposed mechanism for the hydration of  $\text{CO}_2$  by  $[\text{Zn}]$  CA.<sup>6,28</sup>

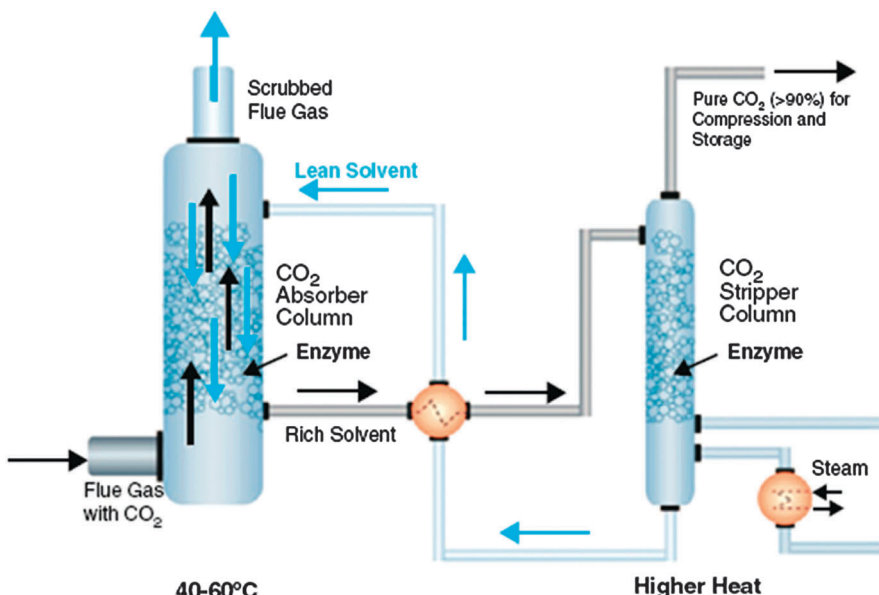


Fig. 10 Schematic of the combination of the CA-catalytic  $\text{CO}_2$  conversion process and chemical absorption process. Reproduced with permission from ref. 2. Copyright 2011 Elsevier.

conducted by Trachtenberg's and Chen's groups.<sup>30,31</sup> The constructed CA "permeator" was mainly composed of two hollow fiber microporous membranes (*i.e.*, the feed fiber membrane and sweep fiber membrane) separated by a CA-containing liquid medium. During the separation process,  $\text{CO}_2$  in the feed gas was diffused to the external surface of the feed fiber membrane, contacted with CA in the liquid medium and then efficiently hydrated into the bicarbonate catalyzed by CA (Fig. S7, ESI†).<sup>31</sup> The generated bicarbonate was subsequently diffused across the matrix of the liquid medium to the outer surface of the sweep fiber membrane, where dehydration of the bicarbonate took place. The acquired  $\text{CO}_2$  was finally released to the sweep fiber membrane. Collectively, the incorporation of CA in the membrane process can enhance the separation efficiency through increasing both the absorption and desorption rates of  $\text{CO}_2$ . This design may offer a mild and efficient alternative for converting and gathering  $\text{CO}_2$  with high purity in comparison to the first case of alkaline scrubbing system. However, there are some serious drawbacks as well, such as the increased operational cost resulting from the requirement for the vacuum condition and the pre-treatment of the feed gas (for removing the membrane-damaged component, *e.g.*,  $\text{SO}_x$  and heavy metals). As a third case for converting  $\text{CO}_2$  into bicarbonate catalyzed by CA, the precipitation/mineralization of the as-formed bicarbonate into water-insoluble  $\text{CaCO}_3$  has also attracted numerous interest. This is primarily ascribed to the following two reasons: (1)  $\text{CaCO}_3$  minerals are physically/chemically stable for thousands of years, averting the release of  $\text{CO}_2$  back to the atmosphere naturally; (2) the mechanical strength and stability of  $\text{CaCO}_3$  minerals make them well-suited as inputs for manufacturing processes or as building-block materials. For instance, Jeong and co-workers<sup>32</sup> firstly accelerated the  $\text{CO}_2$  absorption rate by the sterically-hindered

amine 2-amino-2-methyl-1-propanol (AMP) in the presence of CA, and then converted the absorbed product into  $\text{CaCO}_3$ . The catalytic efficiency ( $k_{\text{cat}}/K_m$ ) and  $\text{CO}_2$  absorption capacities of AMP in the presence or absence of CA were  $2.61 \times 10^6$  or  $1.35 \times 10^2 \text{ M}^{-1} \text{ s}^{-1}$ , and 0.97 or 0.96 mol mol<sup>-1</sup> (AMP), respectively, suggesting a rather positive effect of CA in the  $\text{CO}_2$  absorption process. A further carboxylation process was performed by using various  $\text{Ca}^{2+}$  sources, such as  $\text{Ca(OOCCH}_2\text{CH}_3)_2$  (CAP),  $\text{CaCl}_2$  (CAC) and  $\text{Ca(OOCCH}_3)_2$  (CAA), to produce  $\text{CaCO}_3$  with various polymorphs. Although the CA-catalytic hydration of  $\text{CO}_2$  accelerated the mineralization efficiency, the recycling of CA was difficult to put into use. Considerable effort has been dedicated to addressing this problem. Gu and co-workers<sup>33</sup> reported a CA-assisted approach to synthesize crystalline  $\text{CaCO}_3$  composites accompanied with the *in situ* entrapment of CA. In their work,<sup>33</sup> free CA was primarily utilized as the catalyst for assisting the precipitation/mineralization process, where CA could be *in situ* entrapped in the  $\text{CaCO}_3$  composites. CA immobilized in the  $\text{CaCO}_3$  composites could retain *ca.* 43% activity of its free form. Since  $\text{CaCO}_3$  was pH/temperature sensitive, which may restrict the application of the immobilized CA in some specific areas, other immobilization carriers and protocols were also explored. For instance, Patwardhan and co-workers<sup>34</sup> presented a green approach for the recyclable conversion of  $\text{CO}_2$  to  $\text{CaCO}_3$  catalyzed by CA-encapsulated (bio)inspired silica (Fig. S8, ESI†). Their simple, mild and cost-effective (bio)silicification process for CA immobilization made their protocol easy to scale up for industrial applications. Moreover, the immobilized CA exhibited comparable catalytic activity to free CA, which displayed little enzyme leaching with excellent recycling/storage/thermal stabilities (from Table S2 (ESI†), the ratio of the removed  $\text{CO}_2$  content to the initial content was 86% for the immobilized CA, and 90% for the free CA).

Directly expressing CA onto microorganism cells is an alternative approach to immobilize CA in order to enhance the CO<sub>2</sub> absorption rate and CaCO<sub>3</sub> mineralization efficiency. One typical example of this was proposed by Belcher and co-workers.<sup>35</sup> They constructed an enzymatically-catalyzed CO<sub>2</sub> mineralization process in the bench scale, and modeled/evaluated this at the industrial scale by using standard chemical process scale-up protocols; specifically, a yeast display system from an engineered organism (*Saccharomyces cerevisiae*) was constructed and utilized to screen three CA isoforms (*i.e.*, human CA II, bovine CA II (bCA2) and a CA isoform from *Streptococcus thermophilus*) and several mineralization peptides (*e.g.*, GPA, N66, *etc.*) for investigating their influence on the CO<sub>2</sub> hydration process, CaCO<sub>3</sub> mineralization and on the particle settling rate. Among the several established systems, the bCA2-GPA-yeast system exhibited a much higher rate for all three steps in the bench-scale measurements. Furthermore, an industrial-scale modeling evaluation was also conducted to investigate the cost-effectiveness of this bCA2-GPA-yeast combined system. The modeling result predicted that a process conducted by this bCA2-GPA-yeast combined system was *ca.* 10% more cost effective per tonne of captured CO<sub>2</sub> than a CA-free process. This cost-effectiveness made the process comparable or even favorable to CO<sub>2</sub> capture by the alkaline absorption process. Herein, it should also be noted that, for all three CA-assistant techniques, the rate limiting step is still the mass transfer of CO<sub>2</sub> from the gas phase to water, although the CA-catalyzed process can accelerate this process through increasing the conversion rate of dissolved CO<sub>2</sub> to bicarbonate, followed by further removal or mineralization.

**3.2.2 Conversion of CO<sub>2</sub> to biodegradable chemicals by decarboxylases (*i.e.*, other lyases).** Besides CA, several other types of lyases (decarboxylases) exist in cells and have also been explored for catalyzing the carboxylation of raw materials with CO<sub>2</sub> *in vitro*. The main target of the carboxylation by decarboxylases is to make toxic raw compounds more hydrophilic, thus reducing their affinity toward lipophilic biological components (*e.g.*, membranes, proteins, *etc.*). Interestingly, the decarboxylases do not belong to the enzymes involved in the six major routes of the CO<sub>2</sub> metabolic process and are generally regarded as enzymes that catalyze the decarboxylation processes in cells. Since these decarboxylases can also reversibly catalyze the carboxylation of the substrate with CO<sub>2</sub>, they have gained a lot of attention in the past few years. As summarized by Faber and co-workers,<sup>1</sup> four kinds of enzymatic carboxylation reactions derived from catabolic routes have been developed *in vitro*, including: (1) the carboxylation of epoxides, (2) the carboxylation of aromatics, (3) the carboxylation of hetero-aromatics, and (4) the carboxylation of aliphatics.

Regarding the first route involving epoxides carboxylation, the exploration could be dated back to the 1990s (about 20 years ago). In those cases, cell extracts of *Xanthobacter Py2* or the whole cell rather than purified enzymes were applied for the carboxylation of epoxides (Fig. 11a), but this restricted the further *in vitro* application of this route. In the second route involving aromatics carboxylation, initially, the cell extracts or partially purified phenylphosphate enzymes of *Thauera aromatica* were applied to the carboxylation of phenol with CO<sub>2</sub> to synthesize *p*-hydroxybenzoic acid under ambient conditions. A turnover number of *ca.* 16 000 with a high selectivity toward *p*-hydroxybenzoic acid (~100%) was acquired. Further attempts

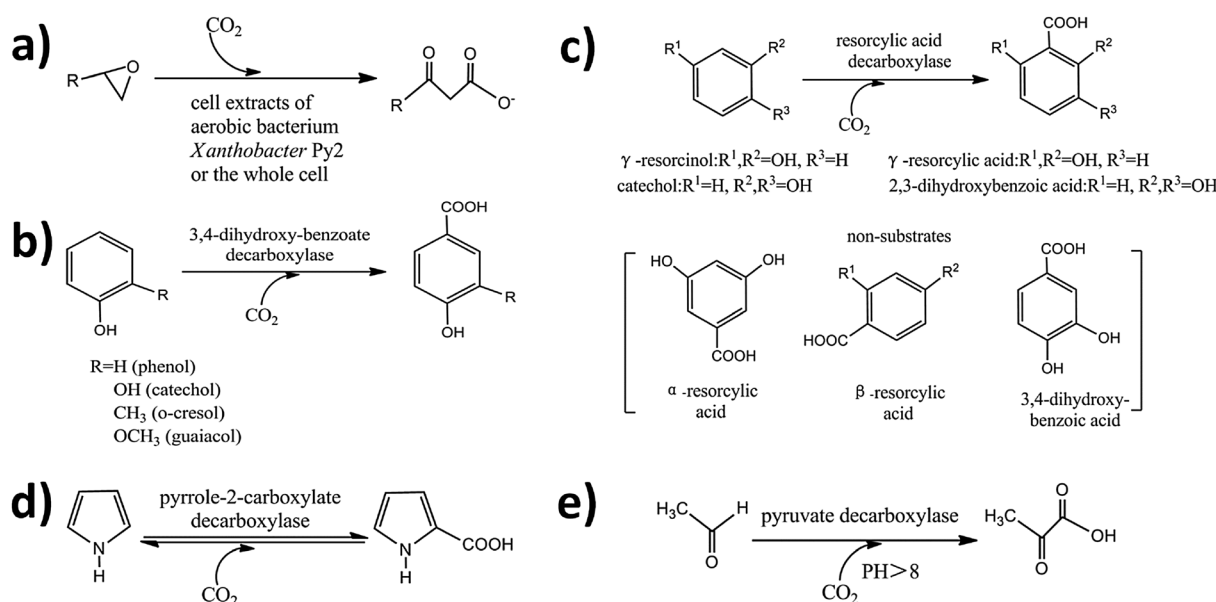


Fig. 11 (a) Biocatalytic carboxylation of epoxides by the cell extracts of the aerobic bacterium *Xanthobacter Py2* or the whole cell; (b) regioselective *para*-carboxylation of non-activated phenolic compounds catalyzed by 3,4-dihydroxy-benzoate decarboxylase; (c) regioselective (*ortho*) carboxylation of non-activated phenolic compounds catalyzed by resorcylic acid decarboxylases; (d) carboxylation of pyrrole by pyrrole-2-carboxylate decarboxylase; and (e) carboxylation of acetaldehyde by pyruvate decarboxylase.<sup>1</sup>

to enhance the enzyme stability were also conducted through immobilizing the enzymes on the low-melting agar.<sup>36</sup> Alternatively, purified 4-hydroxybenzoate decarboxylases from *Chlamy-dophila pneumoniae* AR39, *Enterobacter cloacae* P240109 and *Clostridium hydroxybenzoicum* could also catalyze the reversible carboxylation of phenol with CO<sub>2</sub> to yield 4-hydroxybenzoate. Similar to phenol, catechol could also be reversibly carboxylated into 3,4-dihydroxybenzoate in the presence of bicarbonate catalyzed by 3,4-dihydroxybenzoate decarboxylase from *Clostridium hydroxybenzoicum* (Fig. 11b). Nevertheless, in all the above cases, the equilibrium strongly favoured the decarboxylation (indeed the carboxylation efficiency achieved was no higher than 19%). Besides the regioselective carboxylation in the *para*-position to the phenolic hydroxyl group, some  $\gamma$ -resorcyclic acid decarboxylases (or 2,6-dihydroxybenzoate decarboxylases) from *Agrobacterium tumefaciens*, *Rhizobium radiobacter* and *Rhizobium* sp. have also been used to catalyze the regioselective *ortho*-carboxylation of 1,3-dihydroxybenzene (or  $\gamma$ -resorcinol) with CO<sub>2</sub>. This carboxylation process produced only 2,6-dihydroxybenzoic acid (or resorcyclic acid) without regio-isomeric  $\alpha$ - or  $\beta$ -resorcyclic acid acquired from *meta*-, or *para*-carboxylation (Fig. 11c). In the third route involving hetero-aromatics carboxylation, pyrroles, as another kind of electron-rich hetero-aromatics, were considered as suitable substrates for enzymatic carboxylation. The carboxylation of pyrrole with CO<sub>2</sub> can be catalyzed by pyrrole-2-carboxylate decarboxylase from *Bacillus megaterium* and *Serratia* sp., where an organic acid (such as acetate, propionate, butyrate or pimelate) is adopted as a "cofactor" (Fig. 11d; also the possible reaction mechanism catalyzed by pyrrole-2-carboxylate decarboxylase in the presence of organic acid is proposed as shown in Fig. S9, ESI<sup>†</sup>). In the fourth route involving aliphatics carboxylation, pyruvate decarboxylase from Brewer's yeast was successfully applied for the carboxylation of acetaldehyde with CO<sub>2</sub> to synthesize pyruvate, where thiamine pyrophosphate (TPP) was utilized as a cofactor (Fig. 11e).<sup>37</sup> To acquire high enzymatic activity, operational conditions, especially regarding the pH values, were tailored to manipulate the carboxylation process. As a result, the highest pyruvate yield (81%) was obtained at pH 11 in aqueous sodium bicarbonate buffer that served as both a solvent and CO<sub>2</sub>-source. In order to give a clearer illustration about the extracted/purified enzymes that have been applied for carboxylation, these are listed in Table S3 (ESI<sup>†</sup>) according to previous literature.<sup>1</sup>

## 4. Conversion of CO<sub>2</sub> by a multienzyme system *in vitro*

To synthesize a specific product from CO<sub>2</sub> *in vivo*, cells usually integrate several kinds of enzymes (including the enzyme that directly fixes/converts CO<sub>2</sub> and other enzymes that conduct the subsequent reactions) to implement multienzyme reactions. Additionally, the hierarchical structure and suitable micro-environment of the cells ensure the efficient and ordered processing of a series of catalytic reactions. Enlightened by this,

several multienzyme routes have been developed to produce target fuels/chemicals/materials. This section will describe the state-of-the-art routes to the catalytic conversion of CO<sub>2</sub> by multienzyme systems. Moreover, the existing form of multienzymes in cells also offer efficient and promising ways to construct multienzyme systems *in vitro*, which will also be described in this section.

### 4.1 Conversion of CO<sub>2</sub> to methanol by multiple dehydrogenases

Converting CO<sub>2</sub> into methanol by a multienzyme system has been recognized as one of the most promising possible routes due to the following two attributes: (1) recycling of the "greenhouse" gas, and (2) the efficient production of sustainable/renewable fuel alternatives. In comparison to the fuels (CO, methane, etc.) produced from the single-enzyme route, the liquid methanol produced from the multienzyme reaction has a much higher energy capacity and is easier to transport. For the first time, Yoneyama and co-workers<sup>38</sup> reported the successful electrochemical reduction of CO<sub>2</sub> to methanol with F<sub>ateDH</sub> and methanol dehydrogenase (MDH) as the catalysts and pyrroloquinolinequinone (PQQ) as a cofactor. This approach afforded a facile route for the generation of methanol directly from CO<sub>2</sub> under mild conditions. As described in Yoneyama's report,<sup>38</sup> the type of cofactors greatly influenced the reduction behavior of CO<sub>2</sub>, and the appropriate cofactor can improve the rate of this multienzyme reaction. To take advantage of the fact that dehydrogenases can effectively catalyze the reduction of CO<sub>2</sub> in the presence of a suitable cofactor, Dave and co-workers<sup>39</sup> reported an approach involving the consecutive reduction of CO<sub>2</sub> to methanol with three dehydrogenases as the catalysts and NADH as a cofactor. The overall reaction process is shown in Fig. 12.

As shown in Fig. 12, CO<sub>2</sub> was reduced into formate by F<sub>ateDH</sub> in the first step, followed by the reduction of formate to formaldehyde catalyzed by formaldehyde dehydrogenase (F<sub>aldDH</sub>) in the second step. Methanol was then produced from the reduction of formaldehyde by alcohol dehydrogenase (ADH) in the final step. In all the three steps, NADH acted as a cofactor for each dehydrogenase-catalyzed reduction step. The thermodynamic feasibility of this multienzyme reduction of CO<sub>2</sub> to methanol was investigated by Wang and co-workers.<sup>40</sup> They pointed out that this multienzyme reaction was highly sensitive to the pH value of the reaction medium. The reactions should thus be conducted under the conditions of lower pH values and ionic strength and at elevated temperatures. However, such conditions usually induce denaturation and inactivation of the native enzymes. Thus physicochemical stabilization approaches

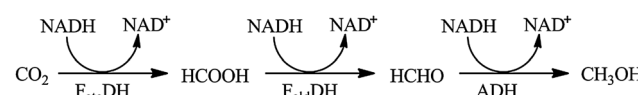


Fig. 12 Reaction route of CO<sub>2</sub> to methanol catalyzed by three dehydrogenases (F<sub>ateDH</sub> – formate dehydrogenase; F<sub>aldDH</sub> – formaldehyde dehydrogenase; ADH – alcohol dehydrogenase).<sup>39</sup>

(*i.e.*, immobilization) should be incorporated. For instance, Dave and co-workers<sup>39</sup> co-encapsulated the three dehydrogenases in a porous silica sol-gel matrix and found that the methanol yield/production was substantially increased compared to that from the free enzymes. They ascribed the enhanced methanol yield/production to the confinement of the multienzyme in the nanopores of silica gels, which favourably alters the reaction thermodynamics and final equilibrium.

With the focus on screening suitable immobilization approaches, Jiang's group carried out a series of investigations on the multienzyme conversion of CO<sub>2</sub> in recent years.<sup>41–44</sup> Different kinds of immobilization approaches and carriers have been designed to create nature-mimicking microenvironments for enzymes. For example, the three dehydrogenases were co-encapsulated in alginate–silica composites. The activity retention and storage stability/reusability of the enzymes were significantly enhanced compared to those of the free enzymes.<sup>41</sup> This phenomenon could be due to the more suitable microenvironment of the alginate–silica composites, including their high hydrophilicity, moderate rigidity and flexibility, optimized cage confinement effect and short diffusion distance. As a relatively novel concept, the biomimetic process can open a promising avenue for enzyme immobilization under mild conditions. By mimicking the biomimetic process, the three dehydrogenases were co-immobilized in TiO<sub>2</sub> nanoparticles using protamine as an inducer under mild conditions. The three dehydrogenases could construct an enzymatic “assembly line” to convert CO<sub>2</sub> into methanol and therefore, a high yield of methanol was obtained.<sup>42</sup> However, co-immobilization of the three enzymes within one support usually suffered from the following limitations: (1) the activities of the enzymes could potentially be influenced by undesirable interactions among the different enzymes; (2) it was difficult to manipulate the immobilization process or the catalytic behavior of the individual enzymes. To allow the sequential reactions to occur within a well-defined reaction zone, a

capsules-in-bead scaffold for the spatially separated multi-enzyme system was constructed.<sup>43</sup> As shown in Fig. 13, the “guest” capsules were prepared through the combination of biomimetic mineralization and layer-by-layer (LbL) assembly by using enzyme-containing CaCO<sub>3</sub> microparticles as sacrificial templates. Afterwards, the “guest” capsules were produced and then co-encapsulated into the larger “host” alginate beads to form the capsules-in-bead scaffold. The three dehydrogenases were located separately in this scaffold and used to convert CO<sub>2</sub> into methanol. Compared with the three dehydrogenases co-encapsulated in an alginate gel bead, the dehydrogenases encapsulated in the capsules-in-bead support showed higher initial activity and enhanced methanol yield. This may be ascribed to the reduced interference among the different enzymes, the elevated local concentration of the intermediate products and the shorter diffusion distance of the intermediate from the active site of one enzyme to another. To further realize the flexible regulation of the individual enzymes and reduce the mass transfer resistance, an ultrathin, hybrid microcapsule was constructed for the multienzyme system to convert CO<sub>2</sub> into methanol through the coupling of biomimetic mineralization and biomimetic adhesion (Fig. 14).<sup>44</sup> Three dehydrogenases of F<sub>ate</sub>DH, F<sub>ald</sub>DH and ADH were immobilized in the capsule lumen, the organic layer of the capsule wall and the silica layer of the capsule wall, respectively. The yield and selectivity of this multienzyme system (71.6% and 86.7%) were remarkably higher than those of the free multienzyme system (35.5% and 47.3%).

As shown in Fig. 12 and as described in the investigations above, the synthesis of one mole of methanol would consume three moles of NADH. However, the high cost of NADH hampers the further application of CO<sub>2</sub> conversion in large-scale operations; therefore, suitable NADH regeneration/reuse strategies are currently being investigated as an important research topic in order to address the above problem. Wang and co-workers<sup>45</sup> investigated the feasibility of methanol production

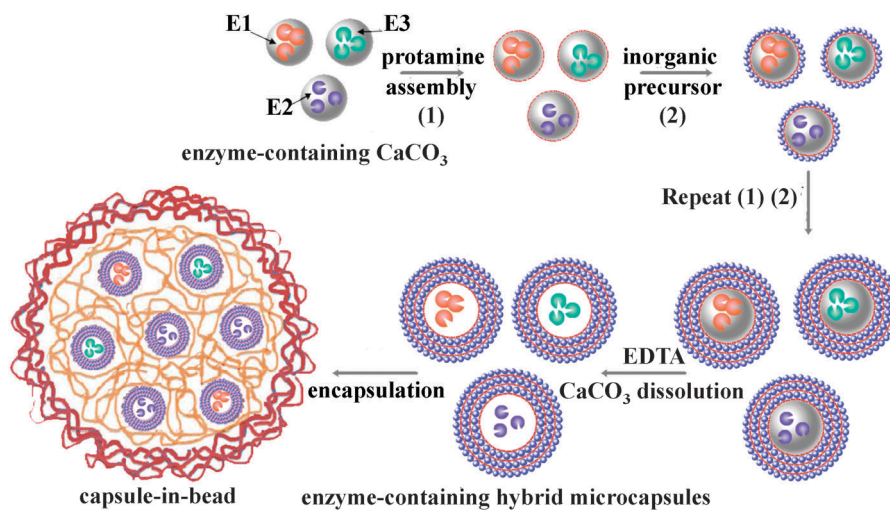
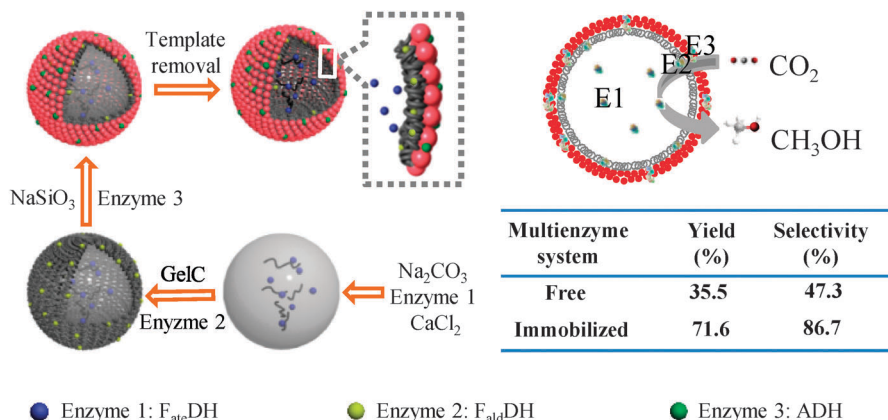
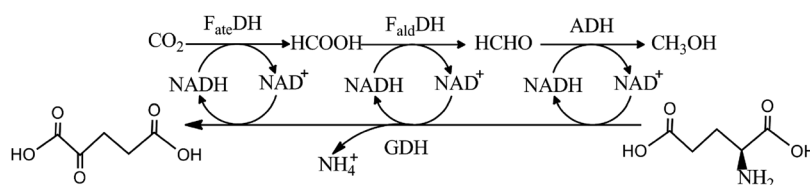


Fig. 13 Schematic of the preparation process of a multienzyme system based on a capsules-in-bead scaffold (E1: F<sub>ate</sub>DH, E2: F<sub>ald</sub>DH, E3: ADH). Reproduced from ref. 43. Copyright 2009 Royal Society of Chemistry.



**Fig. 14** Schematic of the preparation process of a multienzyme system based on an ultrathin, hybrid microcapsule; schematic of the multienzyme reaction of CO<sub>2</sub> to methanol; and the yield and selectivity of the free enzymes and multienzyme system (E1: F<sub>ate</sub>DH, E2: F<sub>ald</sub>DH, E3: ADH). Reproduced from ref. 44. Copyright 2014 American Chemical Society.



**Fig. 15** The multienzyme route for the synthesis of methanol from CO<sub>2</sub> by three dehydrogenases with the *in situ* regeneration of NADH<sup>45</sup> (GDH: glutamate dehydrogenase).

from CO<sub>2</sub> with an *in situ* cofactor regeneration system (Fig. 15). Four enzymes including F<sub>ate</sub>DH, F<sub>ald</sub>DH, ADH and glutamate dehydrogenase (GDH) were co-immobilized on the same particle, while NADH was immobilized on the other particle. GDH was used for the *in situ* regeneration of NADH, driven by the dehydrogenation of glutamate to 2-oxoglutarate. Although the productivity of methanol was lower than that of the free multienzyme system, the immobilized multienzyme system showed fairly good recycling stability. After recycling seven times, more than 80% of its original productivity could be maintained, and the cumulative methanol yield calculated based on the amount of cofactor could reach 127%. Compared to the single-batch yield of 12% in the free multienzyme system, a significant enhancement in cofactor utilization was obtained by using this immobilized multienzyme system. Next, Galarneau and co-workers<sup>46</sup> incorporated another regeneration system to increase the activity of the multienzyme system. They compared three different NADH regeneration systems and found that phosphate dehydrogenase (PTDH) worked most efficiently. The four dehydrogenases (F<sub>ate</sub>DH, F<sub>ald</sub>DH, ADH, PTDH) were then co-encapsulated in phospholipids-silica nanocapsules with an internal diameter of *ca.* 30 nm. After assessment of the catalytic performance of the immobilized multienzyme system, an activity of fifty-five times higher than that of the free multienzyme system could be obtained. All these reports indicated that incorporation of a NADH regeneration system was a useful way to improve the catalytic activity and stability of the multienzyme.

#### 4.2 Conversion of CO<sub>2</sub> to other fuels/chemicals/materials by use of a multienzyme system

Although the conversion of CO<sub>2</sub> to methanol through multiple dehydrogenases offers a promising route for simultaneously consuming CO<sub>2</sub> (greenhouse gas) and acquiring methanol (fuel/chemical), developing novel reaction routes for directly producing advanced fuels/chemicals/materials with higher numbered carbons (>C1) would also be highly competitive.

One encouraging advance that was made by Liao and co-workers is the photosynthetic recycling of CO<sub>2</sub> into isobutyraldehyde (Fig. 16).<sup>47</sup> They genetically engineered *Synechococcus elongatus* PCC7942 through the expression of several key genes (*alsS*, *ilvC* and *ilvD*) to produce isobutyraldehyde from CO<sub>2</sub>. The primary steps for the CO<sub>2</sub> conversion process are shown in Fig. 16, where Rubisco, acetolactate synthase (AlsS), aceto-hydroxy acid isomerase (IlvC), dihydroxy-acid dehydratase (IlvD) and 2-ketoacid decarboxylase (Kdc) were the five key enzymes. Since Rubisco was the bottleneck in carbon fixation in *Cyanobacteria*, an overexpression of this enzyme could increase the reaction rate of CO<sub>2</sub>. Accordingly, the productivity of isobutyraldehyde could be increased. In Liao's work,<sup>47</sup> although several single-enzyme routes were combined for converting CO<sub>2</sub> into target molecules, the multienzyme reaction actually occurred *in vivo* (*Cyanobacteria*) rather than *in vitro*. Inspired by this *in vivo*-engineered CO<sub>2</sub> conversion process, Wendell and co-workers<sup>48</sup> constructed an *in vitro* artificial photosynthesis system through engineering the essential

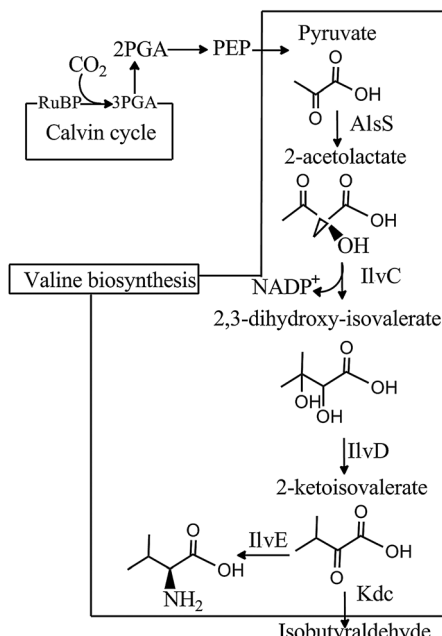


Fig. 16 The multienzyme route for the synthesis of isobutyraldehyde from  $\text{CO}_2$ . AlsS: acetolactate synthase; IlvC: acetohydroxy acid isomerase; IlvD: dihydroxy-acid dehydratase; Kdc: 2-ketoacid decarboxylase.<sup>47</sup>

enzymes in the Calvin cycle and in an ATP-producing photoconversion system (also denoted as BR/ $\text{F}_0\text{F}_1$ -ATP vesicles) into foam architectures (Fig. S10, ESI†). During this process, the Tungara frog surfactant protein (Ranaspumin-2) was required for the coupled enzymes and BR/ $\text{F}_0\text{F}_1$ -ATP vesicles to be concentrated into the Plateau channels of the foam. The artificial photosynthesis system could be successfully utilized for converting  $\text{CO}_2$  into sugars (*e.g.*, glucose) with a conversion ratio of *ca.* 96%. According to the report,<sup>48</sup> the glucose-producing capability of this photosynthesis system was 116 nmol (glucose)  $\text{mL}^{-1} \text{ h}^{-1}$ . It was also assumed that if a foam architecture containing the glucose-producing system was layered to 1 m in height and the conversion ratio of sugar to 2,5-dimethylfuran was 88%, this artificial photosynthesis system could have the capability to produce 10 kg  $\text{ha}^{-1}$  of 2,5-dimethylfuran per hour. Furthermore, supposing that a hectare of foam could receive sunlight for 11 h  $\text{day}^{-1}$ , a productivity of 34.5 t  $\text{ha}^{-1} \text{ a}^{-1}$  of 2,5-dimethylfuran could be achieved, which is ten times higher than that of DMF (3.4 t  $\text{ha}^{-1} \text{ a}^{-1}$ ) from biomass.

Recently, Wang and co-workers<sup>49</sup> explored a relatively simpler multienzyme route for converting  $\text{CO}_2$  and ethanol into L-lactic acid, which denoted a novel and sustainable alternative way to synthesize building blocks for biodegradable polymers. As shown in Fig. 17, the catalytic process mainly consisted of three single-enzyme routes: (1) the oxidation of ethanol to acetaldehyde by ADH in the presence of  $\text{NAD}^+$ ; (2) the synthesis of pyruvate from  $\text{CO}_2$  and acetaldehyde catalyzed by pyruvate decarboxylase; and (3) the reduction of pyruvate to L-lactic acid by lactate dehydrogenase (LDH) in the presence of  $\text{NADH}$ . Obviously, the cycling of  $\text{NAD}^+/\text{NADH}$  could be achieved *via* the first and third single-enzyme route. Another interesting

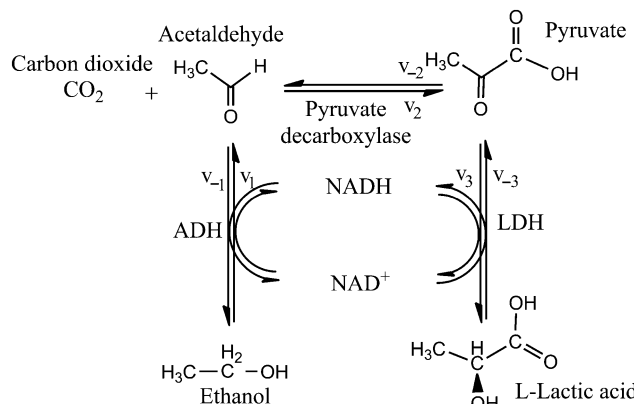


Fig. 17 The multienzyme route for the synthesis of L-lactic acid from  $\text{CO}_2$  and ethanol.<sup>49</sup>

result in their research was that the reaction kinetics for each individual reaction remained unaltered in the multienzyme reaction. Therefore, the kinetic parameters determined from the individual reactions could be directly employed for prediction of the mixed reaction kinetics.

## 5. Future perspectives

Enzymatic conversion for  $\text{CO}_2$  capture, sequestration and utilization provides a green and promising approach to reduce global warming and climate change. Inspired by the  $\text{CO}_2$  metabolic process in cells, two classes of enzymes (oxidoreductases and lyases) have been successfully utilized for converting  $\text{CO}_2$  into different types of fuels/chemicals/materials. To enhance the efficiency of the enzyme catalytic process, various technologies or approaches have been reported for the rational preparation of enzyme-based catalysts, for the optimization of the reaction processes and for the elucidation of reaction mechanisms.

Despite a large number of investigations, significant scientific and technical advances are still required for the large-scale utilization of the enzymatic conversion of  $\text{CO}_2$ . According to the best of our knowledge, the following aspects should be paid more attention in future research: (1) current enzymes are generally expensive and environmentally sensitive catalysts, which hinder their industrial applications. Several approaches up to the bench scale (including enzyme modification and enzyme immobilization) have been developed to reduce the cost and to improve the activity/stability of the enzymes. Screening some of these developed approaches and scaling them up to an industrial level are particularly desired. Furthermore, a recently explored methodology (*i.e.*, *de novo* computational enzyme design) can be used to create novel enzymes with specific properties for efficient  $\text{CO}_2$  conversion, which therefore offers alternative opportunities for industrial application. (2) In the enzymatic conversion of  $\text{CO}_2$ , cofactor-dependent reactions are widely involved. However, the high price and difficult availability of the ion-type cofactor ( $\text{NADH}$  and  $\text{NADPH}$ ) severely restrict large-scale applications. In this tutorial review, we introduced some representative approaches to regenerate

and reuse the cofactors. These existing approaches usually consist of complicated reaction processes or expensive additives (such as a noble metal-based mediator). Quite recently, converting CO<sub>2</sub> into formate by utilizing H<sub>2</sub> as a low-cost and molecule-type “cofactor” was ingeniously proposed by Müller and co-workers. Thus, considerably more research effort will be stimulated in attempts to discover new low-cost and low-energy-input approaches for the regeneration and reuse of the cofactor, or for digging out novel enzymatic routes for the conversion of CO<sub>2</sub> with low-cost and easy-available “cofactors”, or even by exploring cofactor-independent enzymes, such as molybdenum- or tungsten-containing F<sub>ate</sub>DH. (3) Many single-enzyme routes derived from the metabolic process of CO<sub>2</sub> in cells pave the way for CO<sub>2</sub> capture, sequestration and utilization. However, only limited multienzyme routes (CO<sub>2</sub> to methanol, CO<sub>2</sub> to glucose, and CO<sub>2</sub> to L-lactic acid) have been constructed *in vitro*. It is therefore imperative to design a number of enzymatic routes and/or to construct novel multienzyme systems for achieving the sustainable production of fuels/chemicals/materials from CO<sub>2</sub>. (4) The utilization of CO<sub>2</sub> based on chemical, photochemical and electrochemical technologies has great application potential. Thus, it is expected that integrating these routes with the enzymatic route may increase selectivity and productivity. For example, the combination of photo-/electrocatalysis with enzymes for the reduction of CO<sub>2</sub> to formate or CO has been reported by several research groups, including Hirst’s and Armstrong’s groups. These reports raise interesting and important issues about the integration of biocatalysis with other technologies for the efficient conversion of CO<sub>2</sub>. In short, in addition to the chemical, photochemical and electrochemical conversions, the enzymatic conversion of CO<sub>2</sub> has become a viable and promising approach for CO<sub>2</sub> capture, sequestration and utilization. Although it has been explored for many years, much more effort should still be devoted to excavating facile and low-energy routes for CO<sub>2</sub> conversion by the use of cost-effective enzyme-based technologies.

## Acknowledgements

The authors thank the financial support from the National Science Fund for Distinguished Young Scholars (21125627), National Natural Science Funds of China (21406163), and the Program of Introducing Talents of Discipline to Universities (B06006).

## References

- S. M. Glueck, S. Gümüs, W. M. Fabian and K. Faber, *Chem. Soc. Rev.*, 2010, **39**, 313–328.
- C. K. Savile and J. J. Lalonde, *Curr. Opin. Biotechnol.*, 2011, **22**, 818–823.
- M. Aresta, A. Dibenedetto and A. Angelini, *Chem. Rev.*, 2013, **114**, 1709–1742.
- W. Wang, S. Wang, X. Ma and J. Gong, *Chem. Soc. Rev.*, 2011, **40**, 3703–3727.
- E. V. Kondratenko, G. Mul, J. Baltrusaitis, G. O. Larrazabal and J. Perez-Ramirez, *Energy Environ. Sci.*, 2013, **6**, 3112–3135.
- A. M. Appel, J. E. Bercaw, A. B. Bocarsly, H. Dobbek, D. L. DuBois, M. Dupuis, J. G. Ferry, E. Fujita, R. Hille, P. J. A. Kenis, C. A. Kerfeld, R. H. Morris, C. H. F. Peden, A. R. Portis, S. W. Ragsdale, T. B. Rauchfuss, J. N. H. Reek, L. C. Seefeldt, R. K. Thauer and G. L. Waldrop, *Chem. Rev.*, 2013, **113**, 6621–6658.
- G. Fuchs, *Annu. Rev. Microbiol.*, 2011, **65**, 631–658.
- R. K. Thauer, *Science*, 2007, **318**, 1732–1733.
- R. Castillo, M. Oliva, S. Martí and V. Moliner, *J. Phys. Chem. B*, 2008, **112**, 10012–10022.
- M. Beller and U. T. Bornscheuer, *Angew. Chem., Int. Ed.*, 2014, **53**, 4527–4528.
- Y. Amao, N. Shuto, K. Furuno, A. Obata, Y. Fuchino, K. Uemura, T. Kajino, T. Sekito, S. Iwai, Y. Miyamoto and M. Matsuda, *Faraday Discuss.*, 2012, **155**, 289–296.
- R. K. Yadav, J. O. Baeg, G. H. Oh, N. J. Park, K. J. Kong, J. Kim, D. W. Hwang and S. K. Biswas, *J. Am. Chem. Soc.*, 2012, **134**, 11455–11461.
- T. Reda, C. M. Plugge, N. J. Abram and J. Hirst, *Proc. Natl. Acad. Sci. U. S. A.*, 2008, **105**, 10654–10658.
- K. Schuchmann and V. Müller, *Science*, 2013, **342**, 1382–1385.
- Y. Lu, Z. Y. Jiang, S. W. Xu and H. Wu, *Catal. Today*, 2006, **115**, 263–268.
- H. Dobbek, *Coord. Chem. Rev.*, 2011, **255**, 1104–1116.
- A. Bassegoda, C. Madden, D. W. Wakerley, E. Reisner and J. Hirst, *J. Am. Chem. Soc.*, 2014, **136**, 15473–15476.
- J. H. Jeoung and H. Dobbek, *Science*, 2007, **318**, 1461–1464.
- W. Shin, S. H. Lee, J. W. Shin, S. P. Lee and Y. Kim, *J. Am. Chem. Soc.*, 2003, **125**, 14688–14689.
- A. Parkin, J. Seravalli, K. A. Vincent, S. W. Ragsdale and F. A. Armstrong, *J. Am. Chem. Soc.*, 2007, **129**, 10328–10329.
- T. W. Woolerton, S. Sheard, E. Reisner, E. Pierce, S. W. Ragsdale and F. A. Armstrong, *J. Am. Chem. Soc.*, 2010, **132**, 2132–2133.
- T. W. Woolerton, S. Sheard, E. Pierce, S. W. Ragsdale and F. A. Armstrong, *Energy. Environ. Sci.*, 2011, **4**, 2393–2399.
- Y. S. Chaudhary, T. W. Woolerton, C. S. Allen, J. H. Warner, E. Pierce, S. W. Ragsdale and F. A. Armstrong, *Chem. Commun.*, 2012, **48**, 58–60.
- A. Bachmeier, V. C. C. Wang, T. W. Woolerton, S. Bell, J. C. Fontecilla-Camps, M. Can, S. W. Ragsdale, Y. S. Chaudhary and F. A. Armstrong, *J. Am. Chem. Soc.*, 2013, **135**, 15026–15032.
- H. A. Hansen, J. B. Varley, A. A. Peterson and J. K. Nørskov, *J. Phys. Chem. Lett.*, 2013, **4**, 388–392.
- L. C. Seefeldt, M. E. Rasche and S. A. Ensign, *Biochemistry*, 1995, **34**, 5382–5389.
- Z. Y. Yang, V. R. Moure, D. R. Dean and L. C. Seefeldt, *Proc. Natl. Acad. Sci. U. S. A.*, 2012, **109**, 19644–19648.
- K. M. Merz and L. Banci, *J. Am. Chem. Soc.*, 1997, **119**, 863–871.
- S. H. Zhang, H. Lu and Y. Q. Lu, *Environ. Sci. Technol.*, 2013, **47**, 13882–13888.

- 30 M. Trachtenberg, *US Pat.*, US20080003662, 2008.
- 31 Y. T. Zhang, L. Zhang, H. L. Chen and H. M. Zhang, *Chem. Eng. Sci.*, 2010, **65**, 3199–3207.
- 32 M. Vinoba, M. Bhagiyalakshmi, A. N. Grace, D. H. Chu, S. C. Nam, Y. Yoon, S. H. Yoon and S. K. Jeong, *Langmuir*, 2013, **29**, 15655–15663.
- 33 E. T. Hwang, H. Gang, J. Chung and M. B. Gu, *Green Chem.*, 2012, **14**, 2216–2220.
- 34 C. Forsyth, T. W. S. Yip and S. V. Patwardhan, *Chem. Commun.*, 2013, **49**, 3191–3193.
- 35 R. Barbero, L. Carnelli, A. Simon, A. Kao, A. D. Monforte, M. Ricco, D. Bianchi and A. Belcher, *Energy Environ. Sci.*, 2013, **6**, 660–674.
- 36 M. Aresta and A. Dibenedetto, *Rev. Mol. Biotechnol.*, 2002, **90**, 113–128.
- 37 M. Miyazaki, M. Shibue, K. Ogino, H. Nakamura and H. Maeda, *Chem. Commun.*, 2001, 1800–1801.
- 38 S. Kuwabata, R. Tsuda and H. Yoneyama, *J. Am. Chem. Soc.*, 1994, **116**, 5437–5443.
- 39 R. Obert and B. C. Dave, *J. Am. Chem. Soc.*, 1999, **121**, 12192–12193.
- 40 F. S. Baskaya, X. Y. Zhao, M. C. Flickinger and P. Wang, *Appl. Biochem. Biotechnol.*, 2010, **162**, 391–398.
- 41 S. W. Xu, Y. Lu, J. Li, Z. Y. Jiang and H. Wu, *Ind. Eng. Chem. Res.*, 2006, **45**, 4567–4573.
- 42 Q. Y. Sun, Y. J. Jiang, Z. Y. Jiang, L. Zhang, X. H. Sun and J. Li, *Ind. Eng. Chem. Res.*, 2009, **48**, 4210–4215.
- 43 Y. J. Jiang, Q. Y. Sun, L. Zhang and Z. Y. Jiang, *J. Mater. Chem.*, 2009, **19**, 9068–9074.
- 44 X. L. Wang, Z. Li, J. F. Shi, H. Wu, Z. Y. Jiang, W. Y. Zhang, X. K. Song and Q. H. Ai, *ACS Catal.*, 2014, **4**, 962–972.
- 45 B. El-Zahab, D. Donnelly and P. Wang, *Biotechnol. Bioeng.*, 2008, **99**, 508–514.
- 46 R. Cazelles, J. Drone, F. Fajula, O. Ersen, S. Moldovan and A. Galarneau, *New J. Chem.*, 2013, **37**, 3721–3730.
- 47 S. Atsumi, W. Higashide and J. C. Liao, *Nat. Biotechnol.*, 2009, **27**, 1177–1182.
- 48 D. Wendell, J. Todd and C. Montemagno, *Nano Lett.*, 2010, **10**, 3231–3236.
- 49 X. D. Tong, B. El-Zahab, X. Y. Zhao, Y. Y. Liu and P. Wang, *Biotechnol. Bioeng.*, 2011, **108**, 465–469.